Virology 534 (2019) 114–131

Contents lists available at ScienceDirect

Virology

journal homepage: www.elsevier.com/locate/virology

# Whole-gene analysis of inter-genogroup reassortant rotaviruses from the Dominican Republic: Emergence of equine-like G3 strains and evidence of their reassortment with locally-circulating strains

Eric M. Katz[a,b], Mathew D. Esona[b], Naga S. Betrapally[b], Lucia A. De La Cruz De Leon[c], Yenny R. Neira[d], Gloria J. Rey[e], Michael D. Bowen[b,*]

[a] Cherokee Nation Assurance, Contracting Agency to the Division of Viral Diseases, Centers for Disease Control and Prevention, Arlington, VA, USA
[b] Division of Viral Diseases, National Center for Immunization and Respiratory Diseases, Centers for Disease Control and Prevention, Atlanta, GA, USA
[c] Virology Unit, National Public Health Laboratory, Dominican Republic
[d] Pan American Health Organization/World Health Organization, Santo Domingo, Dominican Republic
[e] Pan American Health Organization, Washington, D.C, USA

ARTICLE INFO

*Keywords:*
Group A rotavirus
Equine-like G3 rotavirus
Reassortment
Gastroenteritis
Vaccine

ABSTRACT

Inter-genogroup reassortant group A rotavirus (RVA) strains possessing a G3 VP7 gene of putative equine origin (EQL-G3) have been detected in humans since 2013. Here we report detection of EQL-G3P[8] RVA strains from the Dominican Republic collected in 2014–16. Whole-gene analysis of RVA in stool specimens revealed 16 EQL-G3P[8] strains, 3 of which appear to have acquired an N1 NSP1 gene from locally-circulating G9P[8] strains and a novel G2P[8] reassortant possessing 7 EQL-G3-associated genes and 3 genes from a locally-circulating G2P[4] strain. Phylogenetic/genetic analyses of VP7 gene sequences revealed nine G3 lineages (I–IX) with newly-assigned lineage IX encompassing all reported human EQL-G3 strains along with the ancestral equine strain. VP1 and NSP2 gene phylogenies suggest that EQL-G3P[8] strains were introduced into the Dominican Republic from Thailand. The emergence of EQL-G3P[8] strains in the Dominican Republic and their reassortment with locally-circulating RVA could have implications for current vaccination strategies.

## 1. Introduction

Group A rotaviruses (RVAs) are members of the *Reoviridae* family, and are a ubiquitous pathogen that causes acute gastroenteritis (AGE) resulting in morbidity and mortality in young children (Estes et al., 2013). RVA infection was responsible for an estimated 128,500 deaths among children < 5 years of age throughout the world in 2016 (GBD, 2016 Diarrhoeal Disease Collaborators, 2018; Troeger et al., 2018).

RVAs are characterized by a segmented, double-stranded RNA (dsRNA) genome, composed of 11 genes encoding six structural viral proteins (VP1 to VP4, VP6, and VP7) and five or six non-structural proteins (NSP1 to NSP5/NSP6) (Matthijnssens et al., 2008a). Current genotyping nomenclature incorporates G*x*-P[*x*]-I*x*-R*x*-C*x*-M*x*-A*x*-N*x*-T*x*-E*x*-H*x*, where *x* represents integers that specify the corresponding genotypes of the VP7-VP4-VP6-VP1-VP2-VP3-NSP1-NSP2-NSP3-NSP4-NSP5 genes, respectively (Matthijnssens et al., 2008a). RVAs infecting humans typically possess either the Wa-like genogroup-1 constellation, G*x*-P[*x*]-I1-R1-C1-M1-A1-N1-T1-E1-H1; the DS-1-like genogroup-2 constellation, G*x*-P[*x*]-I2-R2-C2-M2-A2-N2-T2-E2-H2; or the less common AU-1-like genogroup-3 constellation, G*x*-P[*x*]-I3-R3-C3-M3-A3-N3-T3-E3-H3 (Matthijnssens et al., 2008a). The Wa-like and DS-1-like strains share a common origin with porcine and bovine RVAs, respectively, underlining the evolutionary relationship existing among human and animal RVAs (Matthijnssens et al., 2008b). To date, the Rotavirus Classification Working Group (RCWG) recognizes 36 G, 51 P, 26 I, 22 R, 20 C, 20 M, 31 A, 22 N, 22 T, 27 E, and 22 H genotypes among the RVAs that infect humans and animals (https://rega.kuleuven.be/cev/viralmetagenomics/virus-classification/rcwg).

Previous studies indicate that the VP7 gene of human RVAs may derive a G3 genotype from various animal RVAs, such as those detected in feline, canine, porcine, and lapine species (Dóró et al., 2016). Interspecies reassortment(s) derived from zoonotic transmission(s) increase the genetic diversity among circulating RVAs, and are more frequently detected in humans than animal strains (Cowley et al.,

* Corresponding author. Viral Gastroenteritis Branch, Division of Viral Diseases, National Center for Immunization and Respiratory Diseases, Centers for Disease Control and Prevention, Mailstop H18-7, 1600 Clifton Road NE, Atlanta, GA, 30329-4027, USA.
*E-mail address:* mkb6@cdc.gov (M.D. Bowen).

https://doi.org/10.1016/j.virol.2019.06.007
Received 15 March 2019; Received in revised form 12 June 2019; Accepted 12 June 2019
Available online 13 June 2019
0042-6822/ Published by Elsevier Inc.

2016). The segmented structure of the RVA genome facilitates reassortment *in vivo* during co-infection with multiple RVAs, allowing for intra- and inter-genogroup reassortment events (Estes et al., 2013; Cowley et al., 2016). Although RVAs derived from inter-genogroup reassortment(s) occur globally, they generally exhibit decreased evolutionary fitness compared to the parental strains and are selected against in nature (McDonald et al., 2009). Recently, novel DS-1-like inter-genogroup reassortant (IGR) strains possessing genotype constellations G1/2/3/8-P[8]-I2-R2-C2-M2-A2-N2-T2-E2-H2 have emerged and spread among human populations (Dóró et al., 2016; Cowley et al., 2016; Arana et al., 2016; Fujii et al., 2014; Guerra et al., 2016; Hoa-Tran et al., 2016; Komoto et al., 2015, 2016, 2018; Nakagomi et al., 2017; Perkins et al., 2017; Pietsch and Liebert, 2018; Tacharoenmuang et al., 2016; Yamamoto et al., 2014, 2017). Of these, DS-1-like G1P[8] strains exhibit the earliest date of collection (2012) thus far; however, DS-1-like G3P[8] strains have emerged on at least five continents (Asia, Australia, Europe, North America, and South America) since 2013 (Dóró et al., 2016; Cowley et al., 2016; Guerra et al., 2016; Komoto et al., 2016; Perkins et al., 2017). These 'equine-like G3' (EQL-G3) strains possess a VP7 gene of putative equine origin and exhibit the highest genetic similarity with equine RVA strain RVA/Horse-wt/IND/Erv105/2003–2005/G3P[X] ([Erv105], GenBank accession #: DQ981479.1). The earliest reported EQL-G3 strains were detected in children from Japan in 2013 (Cowley et al., 2016; Komoto et al., 2016; Malasao et al., 2015) – strains RVA/Human/JPN/S13-30/2013/G3P[4] and RVA/Human/JPN/S13-45/2013/G3P[4] possessed a G3-P[4]-I2-R2-C2-M2-A2-N2-T2-E2-H2 constellation and may be regarded as the prototype EQL-G3 strains (Malasao et al., 2015). No additional EQL-G3 strains possessing a P[4] have since been reported, but double IGR EQL-G3 strains possessing a novel G3-P[8]-I2-R2-C2-M2-A2-N2-T2-E2-H2 (EQL-G3P[8]) constellation have emerged among human populations spanning the socioeconomic spectrum in Australia, Brazil, Germany, Hungary, Indonesia, Japan, Spain, Taiwan, and the USA, with reports of endemic circulation confirmed in Australia and Brazil (Dóró et al., 2016; Cowley et al., 2016; Arana et al., 2016; Guerra et al., 2016; Komoto et al., 2016, 2018; Perkins et al., 2017; Pietsch and Liebert, 2018; Luchs et al., 2018; Roczo-Farkas et al., 2018; Utsumi et al., 2018). The first EQL-G3P[8] strains were identified in specimens collected in 2013 from Australia and Thailand (Cowley et al., 2016; Komoto et al., 2016). More recently, EQL-G3 reassortant strains were identified in specimens collected in 2016 exhibiting a G3-P[8]-I2-R2-C2-M2-A2-N1-T2-E2-H2 (Guerra et al., 2016; Pietsch and Liebert, 2018) or G3-P[6]-I2-R2-C2-M2-A2-N2-T2-E2-H2 constellation (Utsumi et al., 2018).

In 2004, the Pan American Health Organization (PAHO), in partnership with the World Health Organization, began regional RVA surveillance among Latin America and Caribbean countries to obtain RVA disease-burden data for use when implementing RVA vaccination programs (de Oliveira et al., 2009). The network was initially established with seven countries and expanded to 11 countries by the end of 2007 (de Oliveira et al., 2009). The U.S. Centers of Disease Control and Prevention (CDC) serves as a regional reference laboratory for the network and conducts strain monitoring and genetic characterization of detected RVA strains to assess strain ecology in the post-RVA vaccine introduction era.

Mixed infections with RVA strains have been previously reported from the Dominican Republic (DOM) (Bourdett-Stanziola et al., 2011; Esona et al., 2017) and are a prerequisite for viral reassortment events. Many residents of the DOM experience low-income living conditions, including instances of humans and farm animals living together in the same dwelling (Bourdett-Stanziola et al., 2011). Prior to the introduction of the live-attenuated G1P[8] RVA vaccine Rotarix (RV1: GSK Biologics, Belgium) (O'Ryan, 2007; Chavers et al., 2018) into the DOM's national immunization program (NIP) in 2012 (Pan American Health Organization, 2012; PATH, 2016), an estimated 61.9% of children suffered diarrhea linked to RVA infection (Santos et al., 2016) and surveillance data from the DOM in 2013 revealed that a population of 1,061,290 children < 5 years of age experienced a RVA mortality rate of 9.1 (per 100,000 children) (World Health Organization, 2016). As of 2016, vaccine coverage in the DOM was relatively low (75%) compared with mainland Latin American countries (Chavers et al., 2018); however, a systematic literature review confirmed RVA vaccination to be effective and well tolerated in the Caribbean (Velazquez et al., 2017). Unfortunately, limited RVA genotype data was reported from the DOM during the years prior to vaccine introduction; however, data from 2002 to 2006 revealed that G1P[8] strains predominated among humans (Bourdett-Stanziola et al., 2008, 2011), and surveillance data from 2012 collected from the bordering country of Haiti indicated G1P[8] (29%) and G9P[8] (21%) strains were the predominant genotypes (Esona et al., 2015a).

Analysis of RVA whole-gene sequences from all 11 genes provides valuable data to better understand the contemporary diversity among RVAs resulting from the accumulation of point mutations, gene rearrangement, genetic reassortment, and genetic recombination (Estes et al., 2013; Matthijnssens et al., 2008a; Ramig, 1997). In addition, RVA whole-gene analysis (WGA) facilitates accurate interpretations of the origin of a given strain, and assists in tracing its evolutionary patterns (Matthijnssens et al., 2008a; Ghosh and Kobayashi, 2011). Although the effects of vaccine-induced selective pressure on RVA strain selection remain unclear, previous studies suggest that RVA vaccines exert immunological pressures that influence the diversity of RVAs in contemporary circulation (Roczo-Farkas et al., 2018; Kirkwood et al., 2011; Kirkwood and Roczo-Farkas, 2014; Jere et al., 2018). WGA provides a powerful tool for characterization of circulating RVA strains post-vaccine introduction and identifying the evolutionary processes that lead to the emergence of atypical strains under vaccine pressure (Jere et al., 2018). The purpose of this study was to conduct WGA of RVA-positive surveillance specimens, collected in the DOM during 2014–2016, to thoroughly characterize the circulating strains.

## 2. Materials and methods

### 2.1. Clinical specimens

Stool specimens were collected at two PAHO sentinel surveillance sites in the DOM, the Dr. Robert Reid Cabral Children's Hospital, Santo Domingo Province, and the Dr. Arturo Grullón University Regional Children's Hospital, Santiago Province. Specimens were collected from hospitalized children who presented symptoms concordant with the WHO case definition for RVA gastroenteritis (WHO Coordinated Rotavirus Surveillance Network, 2012). One exception, specimen 3000503714 ([DOM-3714], hereafter study RVA strains are referenced using the format 'DOM-*xxxx*'), was inadvertently collected from a six year child who otherwise satisfied the WHO case definition for RVA gastroenteritis, and was included in the study. Unfortunately, patient RVA vaccination histories were not available for the specimens included in our study. Specimens were screened for RVA antigen by enzyme immunoassay (EIA) at the surveillance site laboratories using the ProSpecT Rotavirus Microplate Assay (Oxoid, Ltd., UK), according to the manufacturer's instructions. Forty-nine EIA confirmed RVA-positive specimens, collected from children during July 21st, 2014 through May 11th, 2015 (2015 season) and July 13th, 2015 through April 28th, 2016 (2016 season), were included in the study. Collected specimens were stored frozen at −20 °C at the surveillance sites until they were shipped on cold packs to the CDC. At the CDC, specimens were briefly stored at 4 °C prior to RNA extraction, and confirmatory testing by EIA for a subset of specimens was conducted using Premier Rotaclone (Meridian Diagnostics, Inc., USA).

### 2.2. RNA extraction for VP7 and VP4 genotyping

For EIA positive stool specimens, viral RNA was extracted from 10%

stool suspensions, prepared using phosphate-buffered saline (PBS). RNA was extracted using the MagMax™-96 Viral RNA Isolation Kit (Life Technologies, USA) on the automated Kingfisher Flex purification system (ThermoFisher Scientific, USA) according to the manufacturer's instructions, with the addition of 2.0 µL of $10^8$ units/µL of MS2 bacteriophage (ZeptoMetrix, USA) internal process control (IPC) to each sample prior to processing (Gautam et al., 2016). The inclusion of an IPC allows for the detection of reverse-transcription polymerase-chain-reaction (RT-PCR) inhibition using a quantitative RT-PCR (qRT-PCR) assay described in section 2.3 (Gautam et al., 2016). All resulting RNA extracts were immediately stored at −80 °C until testing.

A subset of the RNA extracts could not be genotyped initially; these specimens were subjected to an alternate RNA extraction method using the MagNA Pure Compact RNA Isolation Kit (Roche Applied Science, USA) according to the manufacturer's 'RNA isolation from tissue' protocol, aside from minor modifications (Gautam et al., 2016; Esona et al., 2013). In brief, the starting sample (98.0 µL supernatant) was sourced from freshly prepared and homogenized 10% stool suspensions, following centrifugation at 3000 rpm for 10 min to pellet solids. In addition, 2.0 µL of $10^8$ units/µL of MS2 bacteriophage (ZeptoMetrix, USA) IPC was added to each pre-isolation sample, prior to the addition of 250.0 µL of the Tissue Lysis Buffer provided in the kit (Gautam et al., 2016). Samples were extracted on the MagNA Pure Compact System (Roche Applied Science, USA) using the "RNA_Tissue" instrument protocol. All resulting RNA extracts were immediately stored at −80 °C until testing.

### 2.3. VP7 and VP4 genotypes

RVA VP7 and VP4 genotypes were identified and confirmed by a conventional RT-PCR assay and Sanger sequencing. In brief, dsRNA specific to the VP7 and VP4 genes was amplified by multiplexed one-step RT-PCR using the One-Step RT-PCR kit (Qiagen, USA) on either a GeneAMP PCR System 9700 or a Veriti Thermal Cycler (Applied Biosystems, USA) as described previously (Esona et al., 2015b). The resulting RT-PCR products underwent VP7 and VP4 fragment analysis using the DNA 5K Reagent Kit with the DNA 5K/RNA/Charge Variant Assay LabChip on the LabChip® GX instrument (Caliper Life Sciences-Perkin Elmer, USA), according to the manufacturer's instructions. Analytical results were used to identify VP7 and VP4 genotypes. The VP7 and VP4 genotypes identified by RT-PCR were confirmed by Sanger sequencing as described previously (Mijatovic-Rustempasic et al., 2016). In brief, RVA dsRNA specific to the VP7 and VP4 genes was amplified by RT-PCR using primers 9Con1-L with VP7-RDg and con3 with con2, respectively (Freeman et al., 2008; Gentsch et al., 1992), in combination with the One-Step RT-PCR kit (Qiagen, USA) on either a GeneAMP PCR System 9700 or a Veriti Thermal Cycler (Applied Biosystems, USA). Thermal cycling conditions remained as described previously (Mijatovic-Rustempasic et al., 2016), except that the extension step of '1 min at 72 °C' was replaced by '45 s at 72 °C'. The resulting RT-PCR products underwent electrophoresis using SeaKem ME agarose gels (Lonza Group Ltd., Switzerland), gel band excision and purification (QIAquick Gel Extraction Kit, Qiagen, USA), cycle sequencing (BigDye Terminator v3.1 Cycle Sequencing Kit, ThermoFisher Scientific, USA) and bead-based purification (BioMag Carboxyl beads, Bangs Laboratories, Inc. USA) as described previously (Mijatovic-Rustempasic et al., 2012, 2016); except that RT-PCR products underwent electrophoresis in 1.5% SeaKem ME agarose gels (Lonza Group Ltd., Switzerland) in place of 1.0% agarose gels. Automated separation and base-calling of purified cycle sequencing products was conducted using an ABI 3130xl sequencer (Applied Biosystems, USA). The resulting sequence data were analyzed using Sequencher 5.4 software (Gene Codes Corporation, USA), and genotype assignments were determined using the RotaC online classification tool (http://rotac.regatools.be) and the Basic Local Alignment Search Tool (BLAST) to query nucleotide (nt) identities compared to the currently available RVA sequences in the GenBank database (Altschul et al., 1990; Maes et al., 2009).

Specimens that could not be genotyped and confirmed by RT-PCR amplicon analysis and Sanger sequence analysis underwent additional screening for RVA antigen by EIA using Premier Rotaclone (Meridian Diagnostics, Inc., USA), and/or alternative assays according to the manufacturer's instructions or previously described methods, including: a qRT-PCR assay targeting the NSP3 gene to detect amplifiable RVA nucleic acid (Katz et al., 2017); VP7 and/or VP4 genotype-specific singleplexed qRT-PCR assays (Gautam et al., 2016).

### 2.4. Whole-gene sequencing and analysis

The VP7 and VP4 genotype results were used to select a subset of stool specimens for Next Generation Sequencing (NGS), to generate sequence reads for WGA. In brief, viral RNA was extracted from 30% stool suspensions using the MagNA Pure Compact as described in section 2.2, except that the MS2 bacteriophage IPC was not included. RNA extracts were enriched for RVA dsRNA using a LiCl precipitation (Diaz-Ruiz and Kaper, 1978), followed by bead-based RNA purification using Agencourt RNAClean XP reagent (Beckman Coulter Life Sciences, USA) according to the manufacturer's instructions. Sample library preparation was conducted using the NEBNext® Ultra™ RNA Library Prep Kit for Illumina® with NEBNext® Multiplex Oligos for Illumina® Index Primer Sets 1 and 2 (New England BioLabs Inc., USA) on the Illumina MiSeq System using the MiSeq Reagent Kit v2 500-cycles (Illumina Inc., USA) and the standard 250 bp paired-end reads method.

The resulting MiSeq data were analyzed using CLC Genomics Workbench 10.1.1 software ([CLC bio], https://www.qiagenbioinformatics.com/), incorporating a combination of *de novo* assembly and reference-guided assembly methods using the default parameters, to generate contigs and consensus sequences. Study strains yielding CLC bio-assembled sequence reads resulting in 'nucleotide-based RVA whole-gene consensus sequence covering the complete open reading frame' (hereafter referred to as 'ORF sequence') for all 11 genes, were deposited into GenBank under accession numbers: MG652301–MG652356 (VP7 and VP4); MG670591–MG670786 (VP6, VP1, VP2, VP3, NSP1, NSP2, NSP3); and MG701172–MG701227 (NSP4 and NSP5; Table S1).

### 2.5. Genetic analyses

Genetic analyses of ORF sequences were conducted for each gene and for the concatenated ORF sequences using the Molecular Evolutionary Genetics Analysis Version 6.0 software (MEGA6) (Tamura et al., 2013). Using the MUSCLE algorithm with default parameters (Edgar, 2004) embedded within MEGA6, gene-specific multiple-sequence alignments (MSA) were created using the ORF sequences from each study strain along with that of reference strains retrieved from GenBank. The resulting MSAs from each gene were translated to confirm the expected ORF lengths and the amino acid (aa) sequences. Optimal evolutionary models were then identified for each gene-specific MSA using the Model Testing tool within MEGA6, based on the corrected Akaike information criterion (Tamura et al., 2013; Esona et al., 2018; Hurvich and Tsai, 1989). Gene-specific phylograms were constructed using the optimal substitution model, including eight substitution rate categories and bootstrap testing using 1000 replicates to estimate branch support, applied within the Construct/Test Maximum Likelihood Tree tool found in MEGA6. In addition, the shared nt and aa sequence identities among strains were calculated for each gene, using distance matrices prepared using the *p*-distance algorithm in MEGA6. Lastly, the aa sequences within the VP7 antigenic regions (Ciarlet et al., 1997; Dyall-Smith et al., 1986; Nishikawa et al., 1989) were analyzed using the NCBI-based Amino Acid Explorer online tool (https://www.ncbi.nlm.nih.gov/Class/Structure/aa/aa_explorer.cgi?display=0): aa substitutions were categorized as either 'conservative', 'moderate', or

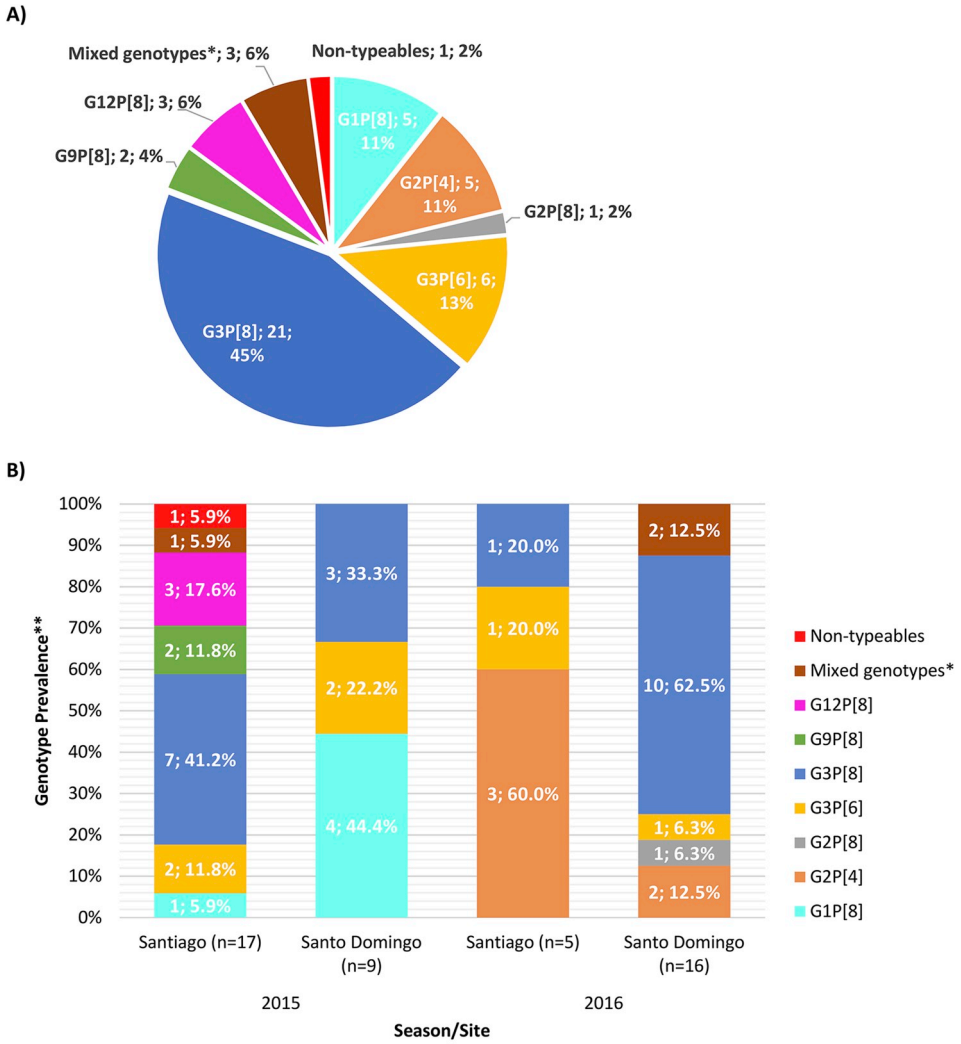


* Includes one G1G3P[6]P[8] and two G2G3P[4]P[8] strains.
** Percentages may not add to 100 due to rounding in individual cells.

**Fig. 1.** The cumulative RVA genotyping results (A) and the genotyping results differentiated by surveillance site and season (B), for RVA-positive specimens collected from the Dominican Republic during 21st July 2014 through 11th May 2015 (2015 season) and 13th July 2015 through 28th April 2016 (2016 season). Non-typeable RVAs are designated GNTP[NT].

'radical' by referencing the aa substitution matrix BLOSUM62 (Henikoff and Henikoff, 1992) scores and changes in the resulting aa chemistry (e.g. molecular charge; chemical bonds; the addition/removal of side chains).

## 3. Results

Of the 49 stool specimens submitted from the DOM to the CDC for genotype identification, 47 were confirmed positive for the detection of RVA and 46 were successfully assigned VP7 and VP4 genotypes using at least two of the molecular assays described previously.

### 3.1. VP7 and VP4 genotypes

The RVA genotyping results from the VP7 and VP4 genes (Fig. 1A) featured: 27 monotypic G3 strains (57%), including 21 G3P[8] strains (45%) and 6 G3P[6] strains (13%); as well as 5 G1P[8] strains (11%) and 5 G2P[4] strains (11%). Results from the 2015 season included: 10 G3P[8] strains (38%); 5 G1P[8] strains (19%); 4 G3P[6] strains (15%); while G9P[8], G12P[8], G1G3P[6]P[8], or non-typeable (GNTP[NT]) strains were identified in lower quantities (Fig. 1B). Results from the 2016 season included: 11 G3P[8] strains (52%), with only 1 G3P[8] strain detected at the Santiago site; 5 G2P[4] strains (24%); while G3P [6], G2P[8], and mixed infection G2G3P[4]P[8] strains were identified in lower quantities (Fig. 1B).

RotaC analyses of partial RVA VP7 sequences (avg. fragment size = 796 bp) confirmed 27 G3P[*x*] strains. The BLAST results from 21 (78%) of these sequences demonstrated ≥99% shared nt sequence identity with EQL-G3 strains previously deposited into GenBank, and 91% shared sequence identity with equine RVA strain Erv105. Seventeen of these study strains were selected for WGA using NGS data; EQL-G3 strains DOM-3722, DOM-3724, DOM-3732, and DOM-3737 lacked the volume of stool required for the NGS assay, and therefore were not analyzed further.

### 3.2. RVA whole-gene analysis

Whole-gene analysis of the NGS data confirmed eight unique genotype constellations including: double (i.e., VP7 and VP4 genes) and triple (i.e., VP7, VP4, and NSP2 genes) IGR EQL-G3P[8] strains; an IGR G2P[8] strain possessing EQL-G3-associated genes and genogroup-2 genes; typical genogroup-1 and genogroup-2 strains; and G1/3-P[6]/

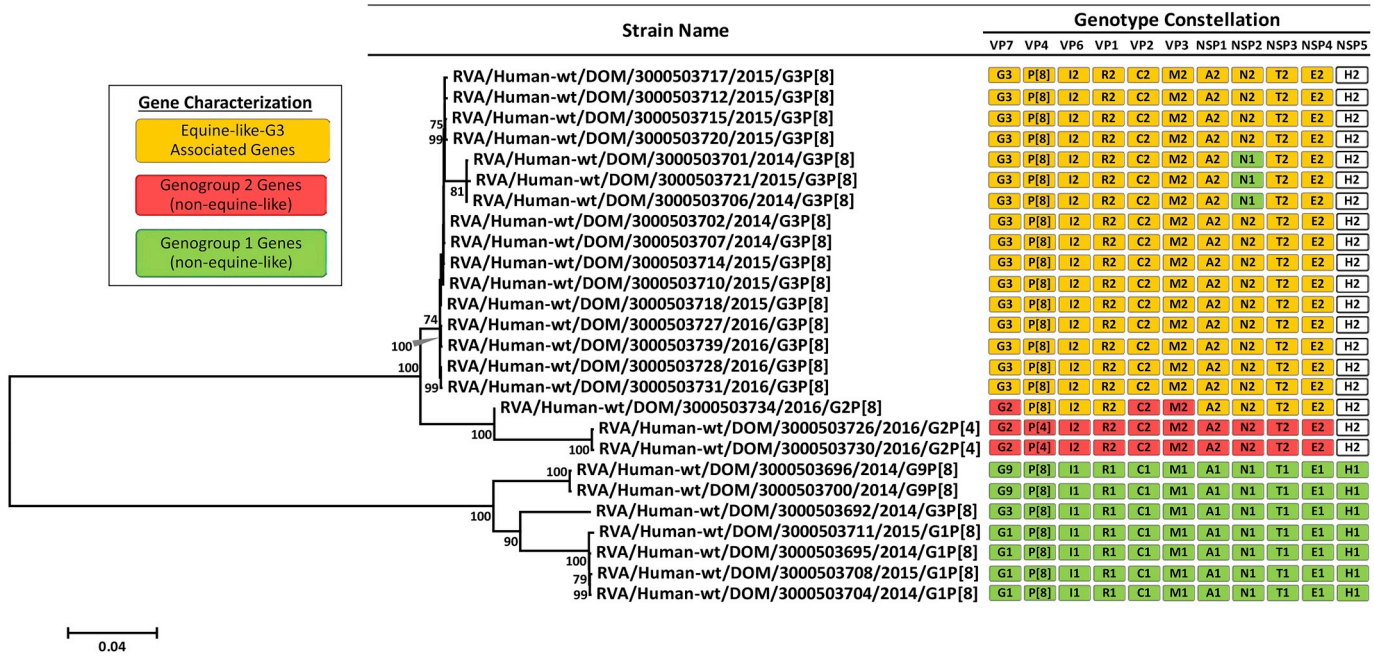


**Fig. 2.** Maximum likelihood phylogram revealing the genetic relatedness of the concatenated, whole-gene ORF sequences (17,545 base pairs) for the 26 monotypic RVA study strains characterized by whole-gene analysis. The strain-specific genotype constellations are included to the right of each strain, and were identified using the assembled ORF sequences. Shape and color coding denotes genotype characteristics. Color coding was not included for the H2 (NSP5) genes that lacked the phylogenetic resolution needed to assign them as EQL-G3-associated or non EQL-G3 genogroup 2 genes. Bootstrap values ≥ 70% are indicated at branch nodes where applicable and the scale bar indicates the number of nucleotide substitutions per site. Mixed genotype specimen 3000503705 was omitted.

[8]-I1/2-R1/2-C1/2-M1/2-A1/2-N1/2-T1/2-E1/2-H1/2 mixed infection strain DOM-3705 (Fig. 2 and Table S1). For analytical purposes, strain DOM-3705 is hereafter differentiated using hypothetical parent strains 'DOM-3705-A' (genogroup-1 backbone) or 'DOM-3705-B' (genogroup-2 backbone) (Fig. 3A–B, 4A–4B, 5A–5D, S1A–S1K and Tables 1 and S1). In addition, the monotypic EQL-G3P[8] study strains and DOM-3705-B are hereafter referred to as the 'DOM-EQL-G3 strains' when describing results universal to this set. A detailed summary of the resulting NGS data from each study strain is included in Table S1.

### 3.3. Sequence identity and phylogenetic analyses

The 'GTR + G' nt substitution model was shown to best fit the RVA NSP4 gene-specific MSA and the concatenated MSA, while the 'GTR + G + I' was shown to best fit the other 10 gene-specific MSAs. Mixed infection strain DOM-3705 was excluded from phylogenetic analyses of the concatenated ORF sequences sourced from the monotypic study strains (17,545 base pairs, Fig. 2). In contrast, genes associated with DOM-3705-A and DOM-3705-B were included in gene-specific phylogenetic analyses and for the calculation of genetic similarities (Fig. 3A–B, 4A–4B, 5A–5D, S1A–S1K and Table 1). Analysis of the concatenated ORF sequences revealed four different RVA strain groups (Fig. 2): the EQL-G3P[8] strains possessing a constellation similar to previously reported EQL-G3P[8] strains; reassortant strains derived from EQL-G3P[8] strains and locally circulating RVA strains (DOM-3701, DOM-3706, DOM-3721, DOM-3734); the non-equine-like genogroup-2 strains; and the genogroup-1 strains (Fig. 2).

The G3 (VP7) ORF sequences from the DOM-EQL-G3 strains and previously reported EQL-G3 strains occupied a distinct and well-supported phylogenetic group (bootstrap value = 100%, Figs. 3A and S1A). The DOM-EQL-G3 sequences shared nt and aa sequence identities of: ≥99.2% nt (≥98.8% aa) among each other; 98.3–99.9% nt (≥97.9% aa) with previously reported EQL-G3 strains; 90.4–91.1% nt (96.9–97.9% aa) with equine strain Erv105; and 81.7–82.1% nt (91.7–92.3% aa) with genogroup-1 G3P[8] study strain DOM-3692 (Figs. 3A and S1A and Table 1). These results along with the G3 diversity observed throughout Figs. 3A and S1A motivated additional analyses to update G3 lineage criteria and the resulting delineations. Preliminary G3 lineages were identified using G3 lineages described by previous studies (Martinez-Laso et al., 2009; Stupka et al., 2009; Chakraborty et al., 2016; Collins et al., 2008); however, multi-parameter metrics were then applied to delineate the G3 lineages reported here (Figs. 3A and S1A and Table 2). In this study the G3 sequences within each described lineage 'occupied a distinct, well-supported monophyletic group (bootstrap support ≥99%)' *and* 'collectively shared ≥89.9% nt identity'; using these criteria G3 lineages I–IX were identified (bootstrap support ≥99%), which exhibited at least 89.9–96.0% shared nt identities (Figs. 3A and S1A and Table 2). Inter-lineage nt homology values ranged from 78.8 to 89.5% when comparing G3 sequences from any two lineages (Table 2). The G3 sequences from the DOM-EQL-G3 strains, previously reported EQL-G3 strains, and the ancestral equine strain Erv105 occupied novel G3 lineage IX (bootstrap = 99%, Figs. 3A and S1A), which diverged into sublineages separating the EQL-G3 strains (bootstrap = 100%) from equine strain Erv105 (Figs. 3A and S1A). In contrast, the G3 sequence from non-EQL-G3 strain DOM-3692 clustered with G3 sequences from previously reported genogroup-1 strains within G3 lineage I (bootstrap = 99%, Figs. 3A and S1A). The inter-lineage aa homology values between strains from G3 lineage IX (almost entirely EQL-G3 strains) and strains from G3 lineages I–VIII ranged from 88.7 to 98.8% resulting in part from inter-lineage aa differences observed within multiple VP7 antigenic sites (Fig. 6 and Table S2). The aa substitutions identified within the VP7 antigenic regions (Ciarlet et al., 1997; Dyall-Smith et al., 1986; Nishikawa et al., 1989) were universally observed at surface exposed residues except for those at aa site 89 (Fig. 6). Relative to the common aa sequence compositions observed among RVA strains from G3 lineages I–VIII, the EQL-G3P[8] study strains exhibited: conservative (site 87) and moderate (DOM-3727 & DOM-3739 at sites 89 & 90, respectively) aa substitutions within antigenic site A; moderate (site 147) aa substitutions within antigenic site B; conservative and moderate (sites 212–213) aa substitutions within antigenic C; and moderate and radical (site 242) aa substitutions within antigenic site F (Fig. 6 and

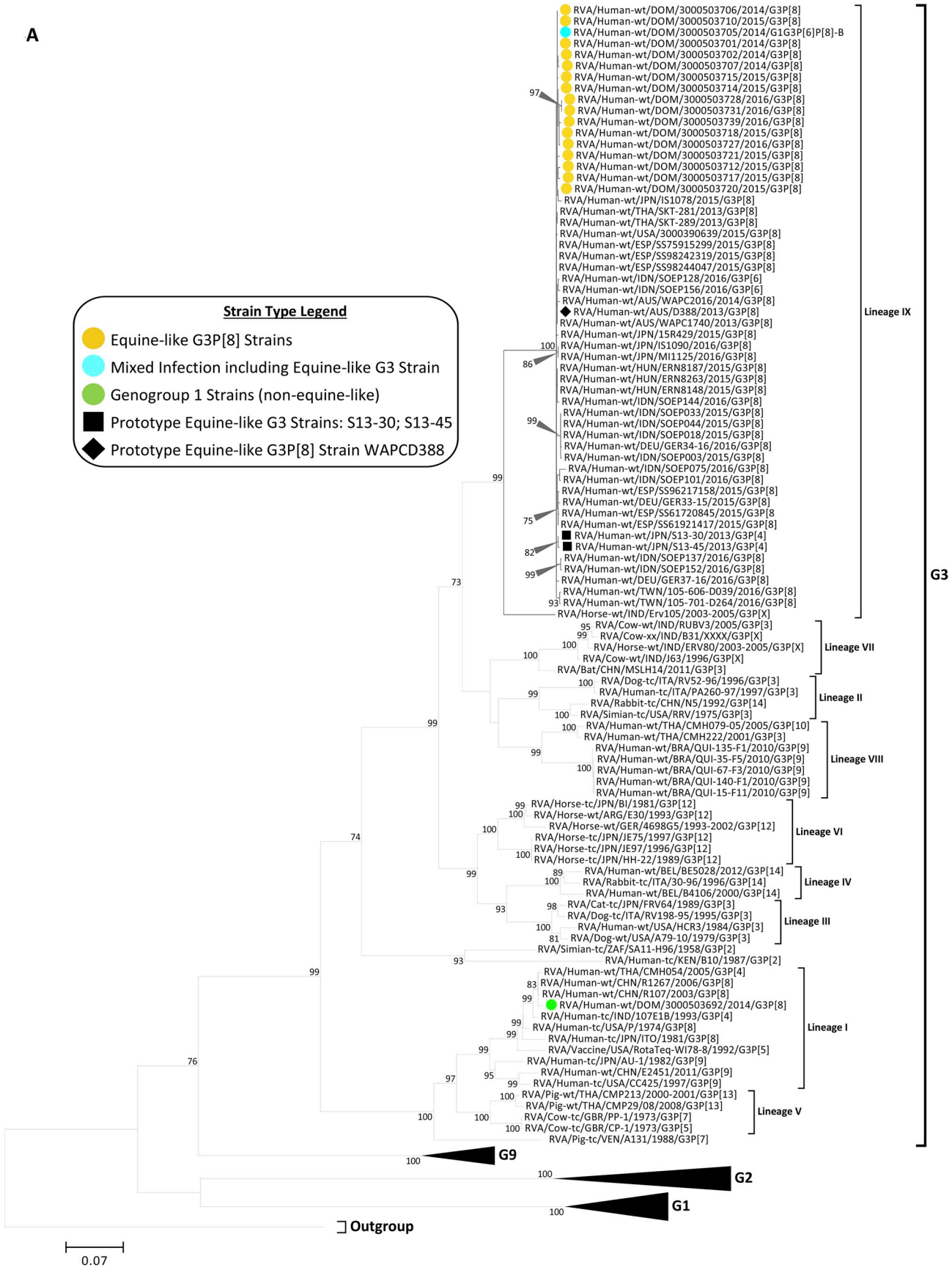


*(caption on next page)*

**Fig. 3.** Maximum likelihood (ML) phylograms (including genetic lineages) revealing the genetic relatedness among the RVA ORF sequences for the VP7 gene, including: A) a phylogram for G3 strains with other G type clades collapsed and B) a phylogram for non-G3 strains with the G3 clade collapsed. Representative RVA strains of known human and animal genotypes were included in addition to the study strains from the Dominican Republic. The shape and color coding of strains for all trees (Fig. 3A–B, 4A–4B, 5A–5D, S1A–S1K) are as indicated in Fig. 3A and B. Bootstrap values ≥ 70% are indicated at branch nodes where applicable and scale bars indicate the number of nucleotide substitutions per site.

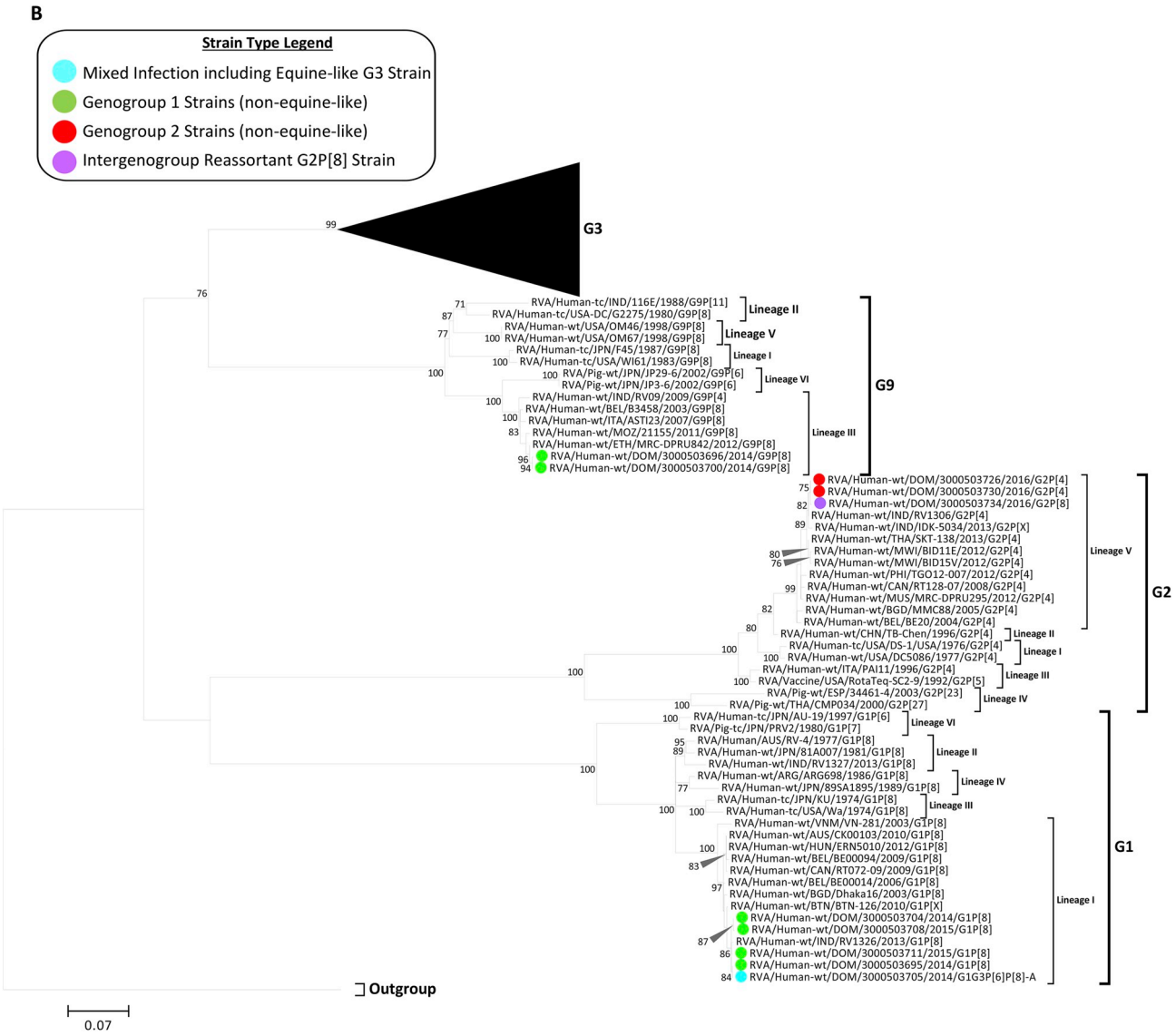


**Fig. 3.** (*continued*)

Table S2).

The G1, G2, and G9 (VP7) ORF sequences from the DOM study strains occupied phylogenetic lineages (Figs. 3B and S1A) that were well resolved using previous lineage descriptions (Stupka et al., 2009; Araujo et al., 2007; Esteban et al., 2010; Ghosh et al., 2011; Khamrin et al., 2007; Le et al., 2010; Mascarenhas et al., 2010; Parra et al., 2005; Phan et al., 2007; Trinh et al., 2010) and therefore additional lineage analyses were not conducted. The G2 sequences from: strains DOM-3726 and DOM-3730; IGR strain DOM-3734; and a subset of previously reported G2P[4] strains, including RVA/Human-tc/USA/DS-1/USA/1976/G2P[4] (DS-1), occupied a monophyletic group (bootstrap = 80%) that diverged to form G2 lineages I, II, and V (Figs. 3B and S1A). Lineage V (bootstrap = 99%, Figs. 3B and S1A) included the sequences from strains DOM-3734, DOM-3726, DOM-3730, and all sequences within this lineage shared 97.8–99.8% nt (≥98.7% aa) identity. In contrast, strains DOM-3734, DOM-3726, and DOM-3730 were genetically less similar (92.8% nt [95.7–96.0% aa]) with strain DS-1 identified in G2 lineage I (Figs. 3B and S1A and Table 1). The G1 sequences from DOM-3705-A and the Wa-like G1P[8] study strains DOM-3704, DOM-3708, DOM-3711, and DOM-3695 clustered with previously reported G1 strains within G1-lineage I (bootstrap = 100%, Figs. 3B and S1A). Lineage I diverged into sublineages, one of which included the four Wa-like study strains above, DOM-3705-A, and RVA/Human-wt/IND/RV1326/2013/G1P[8] (86%, Figs. 3B and S1A), which shared ≥99.5% nt sequence identity.

The P[4], P[6], and P[8] (VP4) ORF study sequences occupied phylogenetic lineages (Fig. 4A–B, S1B) that were well resolved using previous lineage descriptions (Stupka et al., 2009; Araujo et al., 2007; Ghosh et al., 2011; Mascarenhas et al., 2010). All of the P[8] study sequences occupied P[8] lineage III (bootstrap = 100%, Figs. 4A and

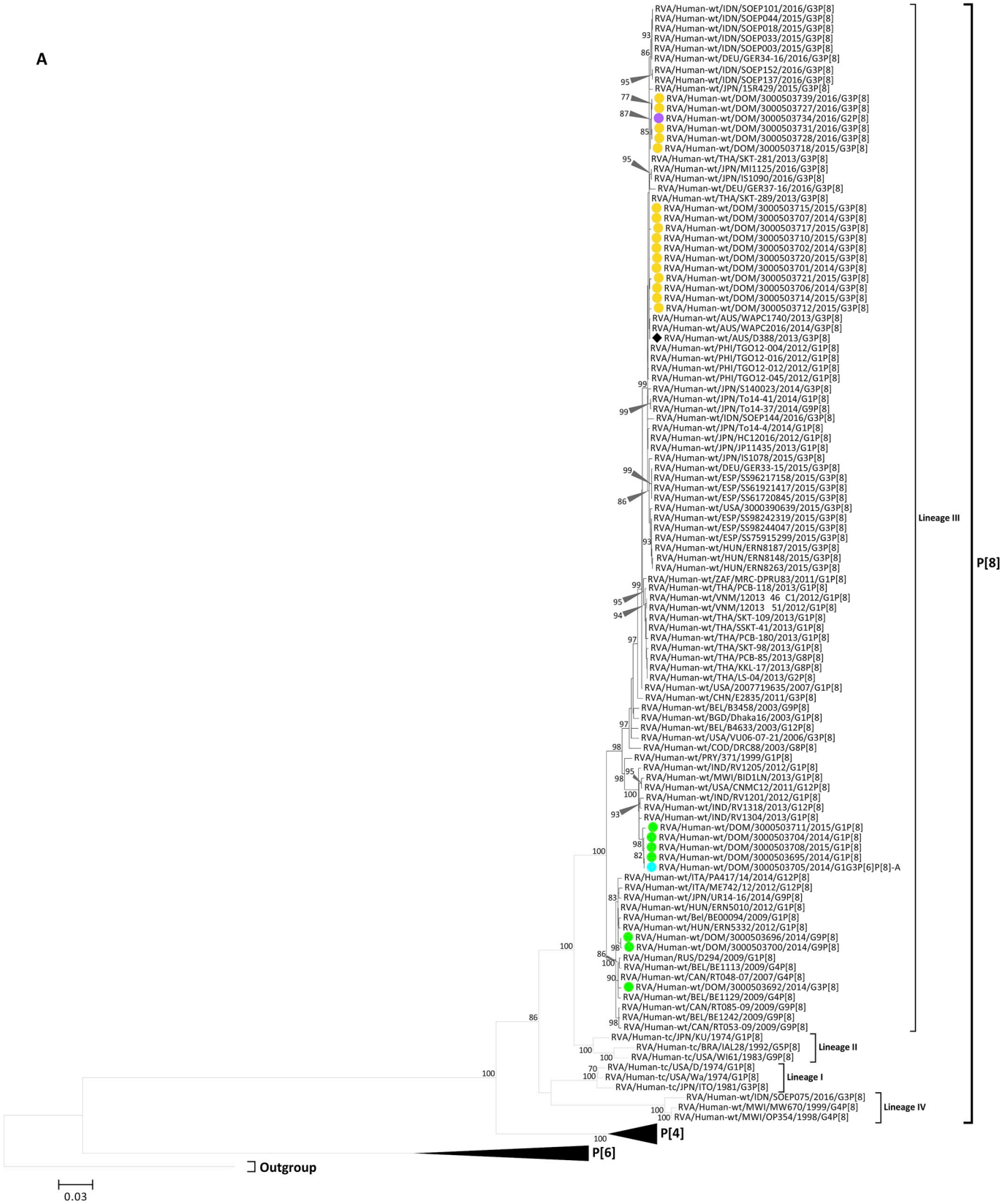


**Fig. 4.** Maximum likelihood (ML) phylograms (including genetic lineages) revealing the genetic relatedness among the RVA ORF sequences for the VP4 gene, including: A) a phylogram for P[8] strains with other P type clades collapsed and B) a phylogram for non-P[8] strains with the P[8] clade collapsed. Representative RVA strains of known human and animal genotypes were included in addition to the study strains from the Dominican Republic. The shape and color coding of strains are as indicated in Fig. 3A–B. Bootstrap values > 70% are indicated at branch nodes where applicable and scale bars indicate the number of nucleotide substitutions per site.

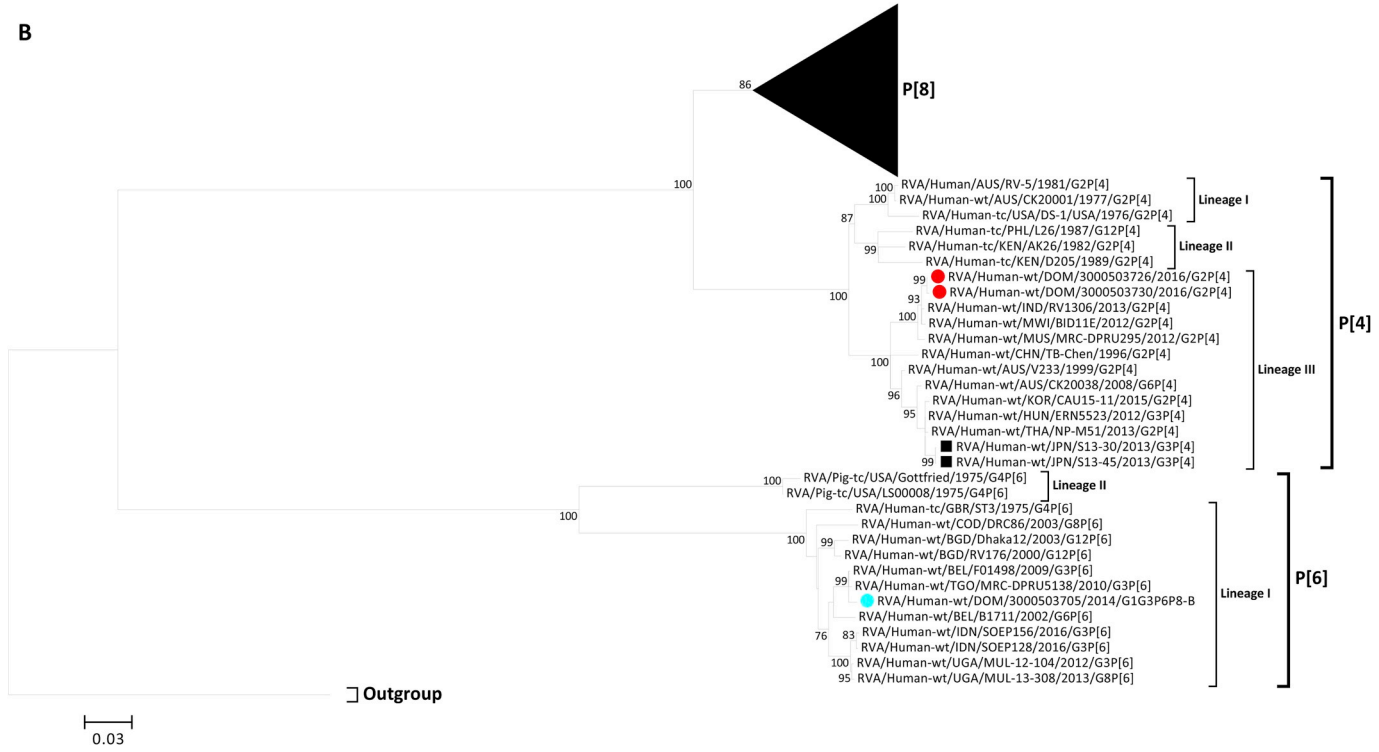


**Fig. 4.** (*continued*)

S1B). Sequences from the monotypic EQL-G3P[8] study strains, previously reported EQL-G3P[8] strains, IGR G2P[8] strain DOM-3734, and additional non-G3 IGR RVAs collected post-2011 all occupied a sublineage of P[8], lineage III (bootstrap = 99%, Figs. 4A and S1B). The P[8] sequences from the EQL-G3P[8] study strains shared sequence identities of: ≥99.6% nt (≥99.5% aa) among each other and 99.1–99.9% nt (≥99.2% aa) with IGR strains within the same sublineage (Figs. 4A and S1B and Table 1); 88.3–88.5% nt (92.9–93.2% aa) with OP354-like, EQL-G3P[8] strain RVA/Human-wt/IDN/SOEP075/2016/G3P[8] (P[8] lineage IV, Figs. 4A and S1B); 95.7–99.9% nt (≥97.7% aa) with the non-EQL-G3 study strains that occupied P[8] lineage III (Figs. 4A and S1B and Table 1); and 90.0–90.2% nt (93.6–93.8% aa) sequence identity with reference strain RVA/Human-wt/USA/Wa/1974/G1P[8] (P[8] lineage I, Figs. 4A and S1B). In contrast to the G3 VP7 gene, the P[8] VP4 gene of the EQL-G3P[8] strains was less phylogenetically distinct from and exhibited greater shared sequence identities with non-EQL-G3P[8] strains (Figs. 4A and S1B and Table 1). Mixed infection strain DOM-3705 possessed sequences encoding P[6]P[8] genotypes (Fig. 4A–B, S1B and Table S1). The P[6] sequence (DOM-3705-B) occupied a sublineage (bootstrap = 76%) that included Indonesian EQL-G3P[6] strains RVA/Human-wt/IDN/SOEP156/2016/G3P[6] and RVA/Human-wt/IDN/SOEP128/2016/G3P[6] (Figs. 4B and S1B). These three sequences shared a sequence identity of 96.7% nt (96.9% aa) and clustered with additional sequences to form P[6] lineage I (100%, Figs. 4B and S1B). Lastly, the VP4 sequences from DOM-3726 and DOM-3730 occupied P[4] lineage III (bootstrap = 100%, Figs. 4B and S1B), and shared 92.7% nt (95.2% aa) sequence identity with lineage I reference strain DS-1 (Figs. 4B and S1B).

The NSP2 ORF sequences from the DOM-EQL-G3 strains encoded 3 N1-associated- and 13 N2-associated-EQL-G3P[8] study strains, as well as N1/N2-associated mixed infection EQL-G3 strain DOM-3705 (Figs. 5A and S1H). Monophyly of the N1 sequences from EQL-G3P[8] study strains DOM-3701, DOM-3706, DOM-3721, previously reported N1-associated-EQL-G3P[8] strains from Brazil and Germany, and all genogroup-1 study strains and DOM-3705-A, was well-supported (bootstrap = 100%, Figs. 5A and S1H). This group diverged into subgroups that separated the Brazilian and German EQL-G3P[8] strains from the other N1 strains (Figs. 5A and S1H). The N1 sequences from DOM-3701, DOM-3706, and DOM-3721 shared the greatest similarity with G9P[8] study strains DOM-3696 and DOM-3700, and monophyly of these strains was well-supported (bootstrap = 99%, Figs. 5A and S1H). The sequences from the N1-associated-EQL-G3P[8] study strains shared sequence identities of: ≥99.9% nt (≥99.7% aa) among each other; 97.3–97.9% nt (98.1–98.7% aa) with previously reported N1-associated-EQL-G3P[8] strains; and ≥97.3% nt (≥98.1% aa) with all other N1-associated study strains (Figs. 5A and S1H and Table 1). Monophyly of the N2 sequences from all other EQL-G3 study strains (including DOM-3705-B); strain DOM-3734; and EQL-G3P[8] strains RVA/Human-wt/THA/SKT-281/2013/G3P[8] (SKT-281) and RVA/Human-wt/THA/SKT-289/2013/G3P[8] (SKT-289) was supported (bootstrap = 80%, Figs. 5A and S1H). This subgroup was nested within a broader group (bootstrap = 74%) that included previously reported N2-associated-EQL-G3 strains; non-G3 IGR strains; and previously reported G2P[4] strains (Figs. 5A and S1H). The N2 sequences from the EQL-G3 study strains shared sequence identities of: ≥99.6% nt (≥99.4% aa) among each other; ≥98.5% nt (≥98.7% aa) with previously reported N2-associated-EQL-G3 strains (Table 1); ≥98.8% nt (≥99.0% aa) with non-G3 IGR strains, including strain DOM-3734; and 98.3–99.1% nt (≥99.0% aa) with the aforementioned G2P[4] strains (Figs. 5A and S1H and Table 1).

The E2 (NSP4) ORF sequences from the DOM-EQL-G3 strains, strain DOM-3734, and a subset of previously characterized EQL-G3 strains occupied a monophyletic subgroup (bootstrap = 95%, Figs. 5B and S1J) that shared ≥98.3% nt (≥96.6% aa) sequence identity. This subgroup was nested within a broader group (bootstrap = 93%) that included Australian bovine-like strains RVA/Human-wt/AUS/RCH272/2012/G3P[14] (RCH272) and RVA/Human-tc/AUS/MG6/1993/G6P (Komoto et al., 2016) (Figs. 5B and S1J). All strains in the above subgroup shared 96.2–97.2% nt (97.7–99.4% aa) sequence identity with strain RCH272. The above sequences exhibited lesser similarity with E2 sequences from a subset of G2P[4] strains, including DOM-3726 and

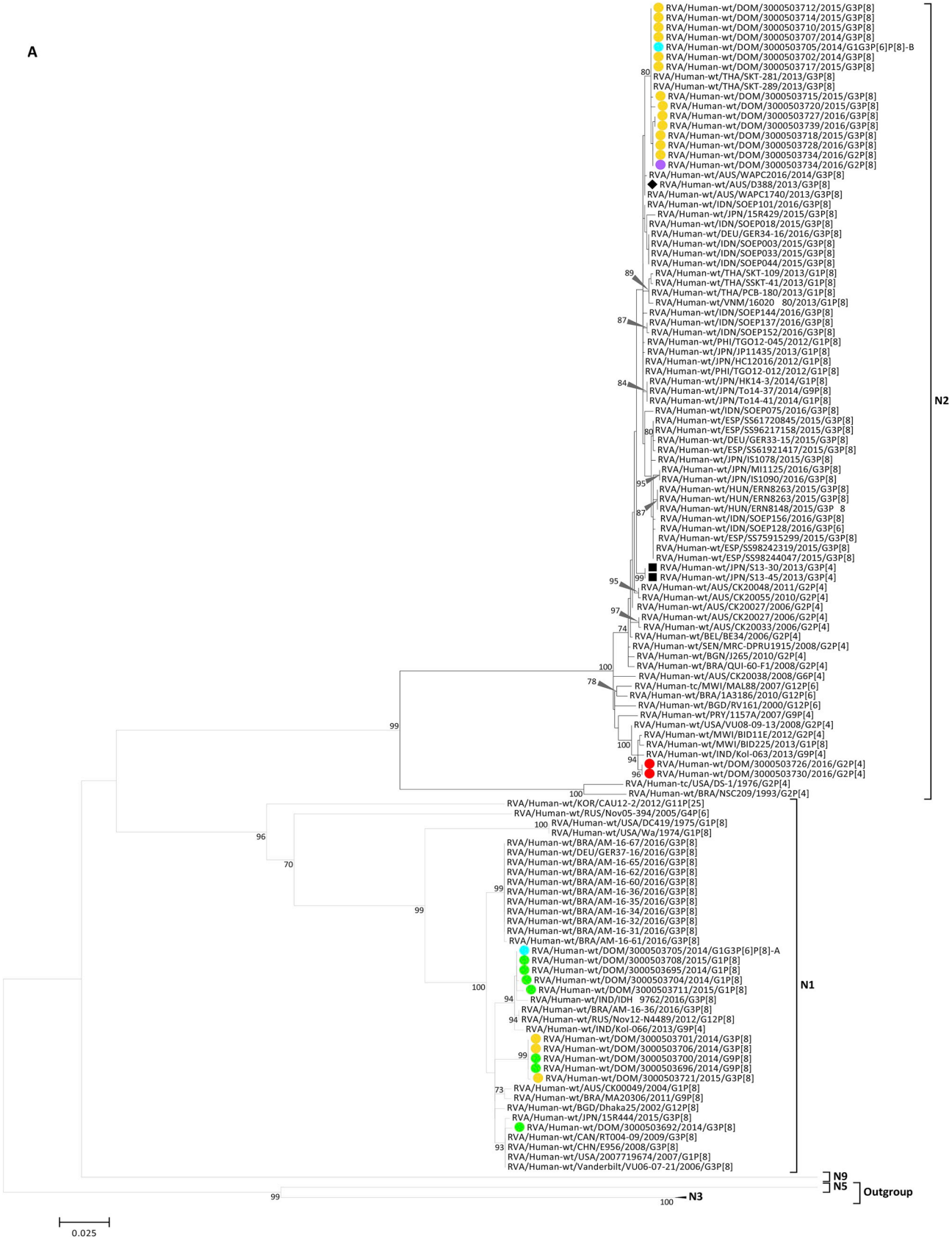


**Fig. 5.** Maximum likelihood phylograms revealing the genetic relatedness among the RVA ORF sequences for genes: A) NSP2, B) NSP4, C) VP2, and D) VP3. Representative RVA strains of known human and animal genotypes were included in addition to the study strains from the Dominican Republic. The shape and color coding of strains are as indicated in Fig. 3A–B. Bootstrap values ≥ 70% are indicated at branch nodes where applicable and scale bars indicate the number of nucleotide substitutions per site.


**Fig. 5.** (*continued*)

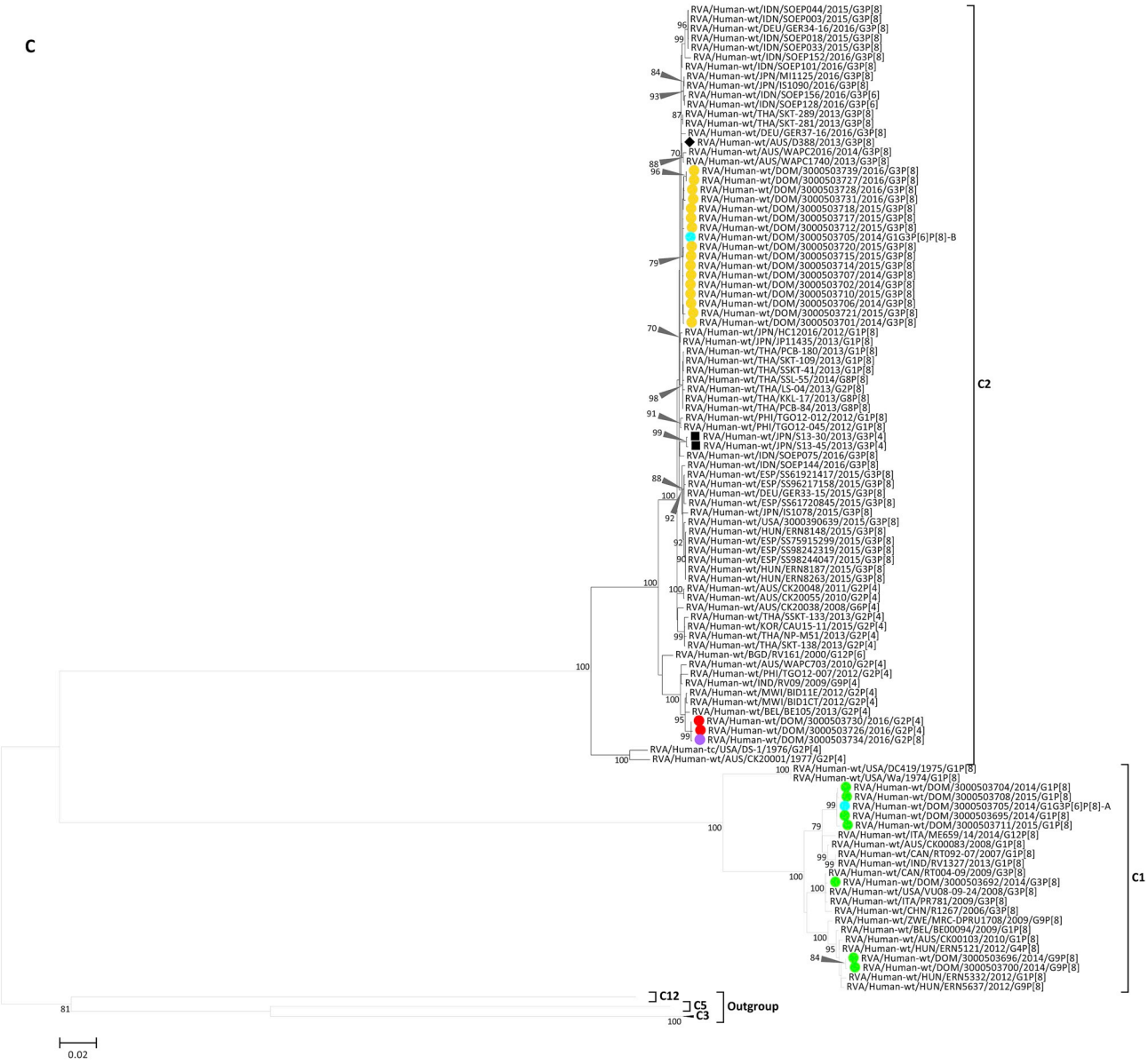


**Fig. 5.** (*continued*)

DOM-3730; previously reported EQL-G3 strains; and a subset of non-G3 IGR strains that occupied a separate and distinct group (bootstrap = 84%, Figs. 5B and S1J). The EQL-G3-associated E2 sequences that occupied the two distinct groups shared 86.6–88.4% nt (92.6–96.0% aa) between each other.

A subset of the VP2 and VP3 sequences from the DOM study strains were divided among two genogroup-2 lineages; interestingly, the sequences from IGR G2P[8] study strain DOM-3734 grouped with G2P[4] study strains DOM-3726 and DOM-3730 rather than the EQL-G3P[8] study strains (bootstrap support ≥ 70%, Fig. 5C–D, S1E–S1F). The VP1, VP6, NSP1, and NSP3 sequences from the DOM study strains also occupied one of two genogroup-2 lineages, but rather separated the DOM-EQL-G3 strains *and* IGR G2P[8] study strain DOM-3734 from the G2P[4] study strains DOM-3726 and DOM-3730 (bootstrap support ≥79%, Figs. S1C–S1D, S1G, S1I). Monophyly of the R2 (VP1) sequences from all EQL-G3 study strains (including DOM-3705-B); strain DOM-3734; and EQL-G3P[8] strains RVA/Human-wt/THA/SKT-281/2013/G3P[8] (SKT-281) and RVA/Human-wt/THA/SKT-289/2013/G3P[8] (SKT-289) was supported (bootstrap = 84%, Fig. S1D). For all six genes, the sequences from the genogroup-1 study strains and DOM-3705-A occupied one of three genogroup-1 lineages, which separated G3P[8] strain DOM-3692; G9P[8] strains DOM-3696 and DOM-3700; and G1P[8] strains DOM-3695, DOM-3704, DOM-3708, DOM-3711, and DOM-3705-A (bootstrap support ≥81%, Fig. 5C–D, S1C–S1G, S1I).

The H2 (NSP5) ORF sequences from the DOM-EQL-G3 strains; strain DOM-3734; previously reported EQL-G3 strains; a subset of non-G3 IGR strains; and previously reported G2P[4] strains, including RVAs identified in Australia and Southeast Asia as early as 1999, occupied a monophyletic subgroup (bootstrap = 73%, Fig. S1K). Monophyly of these strains with additional G2P[4] strains, including DOM-3726 and DOM-3730, was well supported (bootstrap = 97%, Fig. S1K).

## 4. Discussion

Despite vaccine mediated decreases in the global burden of RVA (GBD, 2016 Diarrhoeal Disease Collaborators, 2018; Troeger et al., 2018), continued global RVA surveillance remains important to document and characterize strains in contemporary circulation. RVA surveillance data are essential for future studies investigating RVA vaccine effectiveness (Velazquez et al., 2017), and the increasingly apparent

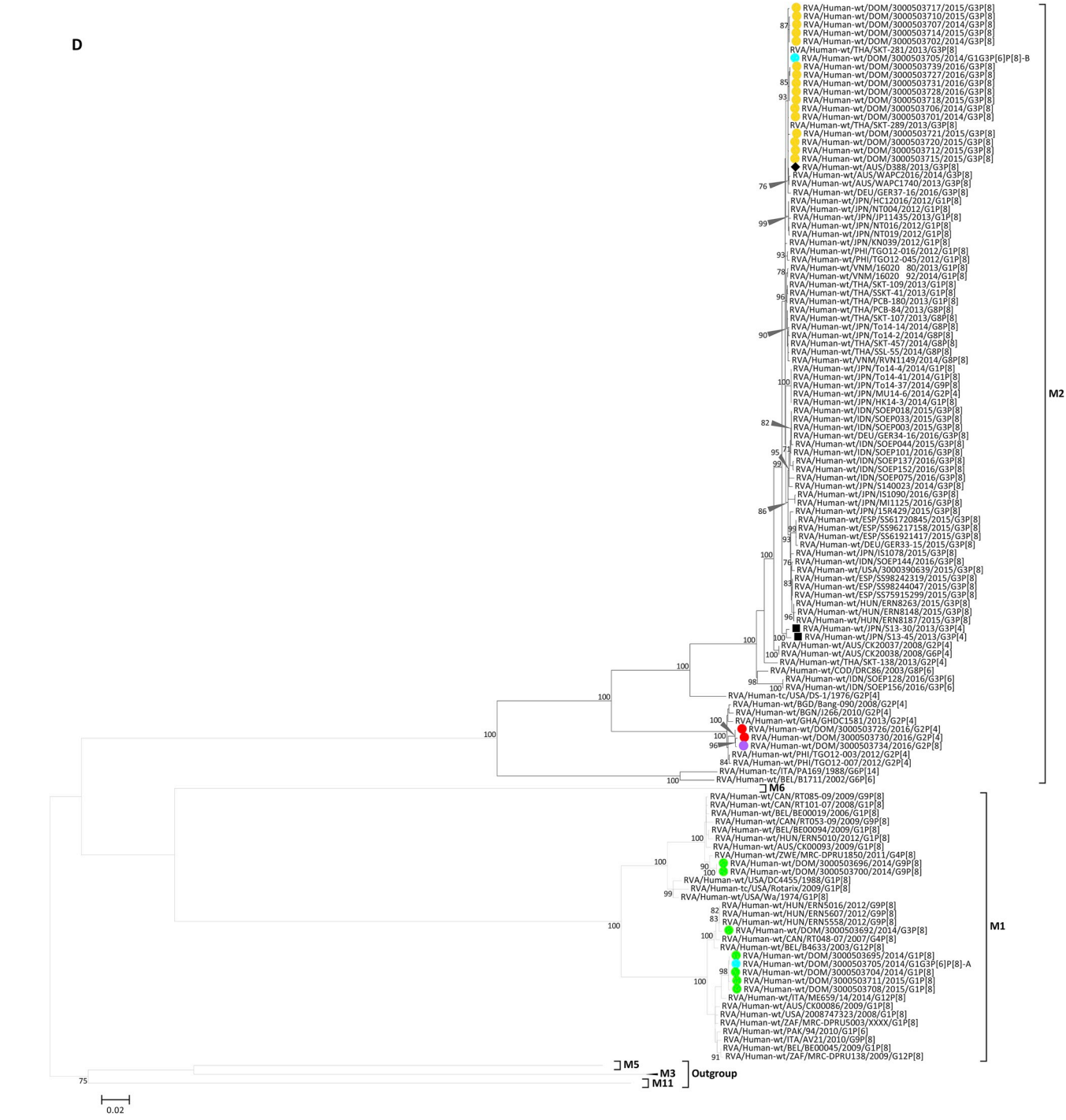


**Fig. 5.** (*continued*)

effects of vaccine-induced strain selection on local strain ecology (Roczo-Farkas et al., 2018; Kirkwood et al., 2011; Kirkwood and Roczo-Farkas, 2014; Jere et al., 2018). From WGA of surveillance specimens collected two to four years post-introduction of Rotarix into the DOM's NIP (Pan American Health Organization, 2012; PATH, 2016), our results confirmed novel IGR EQL-G3P[8] strains that possessed VP7 sequences of putative equine origin (Cowley et al., 2016; Komoto et al., 2016; Malasao et al., 2015) that occupied novel G3 lineage IX (Figs. 3A and S1A), EQL-G3-associated VP4 genes that occupied P[8] lineage III (Figs. 4A and S1B) (Araujo et al., 2007), and a DS-1-like genetic backbone composed of seven or eight EQL-G3-associated genes (Fig. 2). Our findings indicate EQL-G3P[8] strains emerged in the DOM no later than November 2014 and predominated the 2015 and 2016 RVA seasons (Fig. 1). The EQL-G3P[8] study sequences and those described previously were highly conserved across all 11 genes, aside from EQL-G3P[8] strains derived from local reassortment events (e.g. DOM-3701, DOM-3706, and DOM-3721; Figs. 2, 3A,4A and 5A–5D, S1A–S1K and Table 1). Our results also revealed a novel IGR G2P[8] strain possessing seven EQL-G3-associated genes and three genes from a locally-circulating G2P[4] strain, an EQL-G3 mixed infection, and RVA strains possessing typical genogroup-1 or genogroup-2 genotype constellations (Figs. 2, 3A–3B, 4A–4B, 5A–5D, S1A–S1B and Table S1).

Genetic analyses indicate that the EQL-G3P[8] study strains and those described previously share a common origin with DS-1-like G1P

**Table 1**
Summary of observed sequence identities among the ORF sequences of each homologous genotype[a].

| RVA Strains Compared (group A *with* group B) | Shared Sequence Identity (%) | Gene (genotype) | | | | | | | | | | |
|---|---|---|---|---|---|---|---|---|---|---|---|---|
| | | VP7 (G3) | VP4 (P[8]) | VP6 (I2) | VP1 (R2) | VP2 (C2) | VP3 (M2) | NSP1 (A2) | NSP2[f] (N1) | NSP2[f] (N2) | NSP3 (T2) | NSP4 (E2) | NSP5 (H2) |
| **Among EQL-G3 Study Strains** | *Nucleotide Identity* | ≥ 99.2 | ≥ 99.6[e] | ≥ 99.4 | ≥ 99.5 | ≥ 99.6 | ≥ 99.7 | ≥ 99.5 | ≥ 99.9 | ≥ 99.6 | ≥ 99.2 | ≥ 99.2 | ≥ 99.7 |
| | *Amino Acid Identity* | ≥ 98.8 | ≥ 99.5[e] | ≥ 99.4 | ≥ 99.4 | ≥ 99.5 | ≥ 99.6 | ≥ 99.2 | ≥ 99.7 | ≥ 99.4 | ≥ 99.0 | ≥ 98.8 | ≥ 99.0 |
| **EQL-G3 Study Strains *with* Previously Reported EQL-G3 Strains** | *Nucleotide Identity* | 98.3–99.9 | ≥ 95.7 | 95.7–99.9 | 98.6–99.9 | 99.2–99.9 | ≥ 96.6 | 98.4–99.9 | 97.3–97.9[g] | ≥ 98.5 | ≥ 97.2[g] | ≥ 87.1[g] | 99.0–99.8[g] |
| | *Amino Acid Identity* | ≥ 97.9 | ≥ 97.7 | 98.0–99.8 | 99.0–99.9 | ≥ 99.4 | ≥ 97.6 | ≥ 97.9 | 98.1–98.7[g] | ≥ 98.7 | ≥ 97.1[g] | ≥ 93.7[g] | 97.5–99.5[g] |
| **EQL-G3 Study Strains *with* non-EQL-G3 Study Strains** | *Nucleotide Identity* | 81.7–82.1[d] | 95.7–99.9 | ≥ 97.5 | 94.1–99.9 | 97.1–97.4 | 87.2–87.6 | 97.6–99.9 | ≥ 97.3 | ≥ 96.8 | ≥ 96.5 | ≥ 87.5 | ≥ 98.7 |
| | *Amino Acid Identity* | 91.7–92.3[d] | ≥ 97.7 | ≥ 98.9 | 97.9–99.9 | 99.3–99.7 | 92.7–93.3 | ≥ 97.3 | ≥ 98.1 | ≥ 98.1 | ≥ 98.4 | ≥ 94.3 | ≥ 99.0 |
| **WAPCD388-like EQL-G3 Strains[b] *with* Intergenogroup Reassortant Strains[c]** | *Nucleotide Identity* | N/A | 99.1–99.9 | 98.7–99.4 | 98.9–99.8 | 99.4–99.8 | 98.8–99.8 | 98.8–99.9 | N/A | 98.6–99.9 | 97.3–99.9 | N/A | ≥ 99.2 |
| | *Amino Acid Identity* | N/A | ≥ 99.2 | 98.7–99.5 | 99.4–99.9 | ≥ 99.5 | 98.6–99.9 | 97.9–99.8 | N/A | ≥ 98.4 | ≥ 97.8 | N/A | ≥ 98.5 |

[a] Sequence identity values calculated using the p-distance algorithm in MEGA6.
[b] Included EQL-G3 strains that clustered with P[8]-containing EQL-G3P[8] prototype strain WAPCD388 in a supported clade (bootstrap support ≥ 70%), in the resulting phylograms generated in this study.
[c] Included G1P[8]/G9P[8]/G8P[8] strains, possessing a genogroup 2 backbone, that were collected post-2011 and that clustered with EQL-G3P[8] prototype strain WAPC1740 in a distinct and supported clade (bootstrap support ≥ 70%), in the resulting phylograms generated in this study. Does not include G2P[8] study strain DOM-3734.
[d] Comparison of EQL-G3 study strains with Wa-like strain RVA/Human-wt/DOM/3000503692/2014/G3P[8].
[e] Resulting values exclude P[8] from mixed infection strain RVA/Human-wt/DOM/3000503705/2014/G1G3P[6]P[8].
[f] Shared sequence identity values based solely on strains with the same genotype.
[g] Comparisons allowed for the inclusion of 10 EQL-G3 strains identified in Brazil (gene sequences with the complete ORF, previously deposited into the GenBank database).

[8] strains (Figs. 4A, 5A–5D, S1B–S1K and Table 1). These atypical IGR strains appear to have emerged around the same time in Southeast Asia and/or Australia (Cowley et al., 2016; Fujii et al., 2014; Komoto et al., 2015, 2016; Yamamoto et al., 2014, 2017) and exhibited conserved sequences at the VP1–VP4, VP6, NSP1–NSP3, and NSP5 genes (Figs. 4A, 5A, 5C–5D, S1B–S1I, S1K and Table 1). The currently available data indicate that the DS-1-like G1P[8] strains predate the EQL-G3P[8] strains; therefore, the prototype EQL-G3P[8] strain may have been derived from reassortment of an unknown novel G3 strain and a DS-1-like G1P[8] strain. However, further study is required to elucidate the mechanisms and origins associated with the EQL-G3P[8] strains. Nevertheless, the EGL-G3P[8] strains and the DS-1-like G1P[8] strains were also genetically similar to a subset of G2P[4] strains at the VP2–VP3, VP6, NSP1–NSP3, and NSP5 genes, including G2P[4] strains circulating in Australia and Southeast Asia during the post-vaccine introduction era (Figs. 5A, 5C–5D, S1C, S1E–S1H, S1K and Table 1). Therefore, one or both types of these atypical IGR strains were partially derived from G2P[4] strains in contemporary circulation in the geographic area of origin, and both the DS-1-like G1P[8] and EQL-G3P[8] strains share a common origin with these G2P[4] strains.

Atypical EQL-G3P[8] strains were likely introduced into the DOM from another country through virus dispersal of highly conserved EQL-G3P[8] strains. The monotypic EQL-G3P[8] study strains and in many cases those previously reported (Dóró et al., 2016; Cowley et al., 2016; Arana et al., 2016; Guerra et al., 2016; Komoto et al., 2016, 2018; Perkins et al., 2017; Pietsch and Liebert, 2018; Luchs et al., 2018; Roczo-Farkas et al., 2018; Utsumi et al., 2018) exhibit and share unique genetic constellations and conserved sequences distinct from all other RVA strains reported thus far (Figs. 2, 3A, 5A–5D, S1A, S1C–S1H, S1J and Table 1). Excluding the NSP2 genes from DOM-3701, DOM-3706-, DOM-3721 (Fig. 2), the monotypic EQL-G3P[8] study strains and many of those previously reported from multiple geographic locations were highly genetically similar across all 11 genes (Figs. 3A, 4A, 5A–5D, S1A–S1K and Table 1). The resulting phylograms, particularly the VP1 and NSP2 genes, suggest the EQL-G3P[8] study strains are most similar to previously reported EQL-G3P[8] strains SKT-281 and SKT-289 from Thailand (Figs. 5A, S1D, S1H). These two strains predate the EQL-G3P[8] study strains, and therefore may be the source of the EQL-G3P[8] strains emergent in the DOM. Regardless, our results indicate that EQL-G3P[8] strains were more likely introduced into to the DOM from elsewhere, versus derivation solely from strains local to the DOM; especially when considering the novel and distinct nature of the EQL-G3 sequence. Our results also corroborate the previous suggestion of a globally co-circulating pool of highly conserved EQL-G3P[8] strains (Pietsch and Liebert, 2018).

Highly conserved EQL-G3P[8] strains appear to be spreading to new areas; our results also show that EQL-G3P[8] strains can reassort with local genogroup-1 and genogroup-2 RVA strains resulting in novel EQL-G3 reassortants (Figs. 5A and S1H). The N1 sequences from DOM-3701, DOM-3706, DOM-3721 were genetically distinct from previously reported N1-associated EQL-G3P[8] strains (Figs. 5A and S1H), rather these study strains exhibited the greatest genetic similarity with the N1 sequences from locally circulating G9P[8] strains (Figs. 5A and S1H and Table 1). Therefore, these novel triple IGR EQL-G3P[8] study strains were derived from reassortment of an EQL-G3P[8] strain and G9P[8] strain in local circulation (Figs. 5A and S1H and Table 1). Thus far, multiple studies have reported EQL-G3P[8] strains exhibiting a N1 genotype at the NSP2 gene (Guerra et al., 2016; Pietsch and Liebert, 2018), indicating an increased probability of reassortment at the NSP2 gene among EQL-G3 strains relative to the rest of the genetic backbone. A similar phenomena has been reported among recently emergent DS-1-like G1P[8] strains (Jere et al., 2018). The above reassortment events were all reported from countries known to use Rotrarix, therefore the NSP2 gene may serve as a valuable marker for monitoring vaccine-triggered changes to the rotavirus landscape. Novel IGR G2P[8] strain DOM-3734 possessed seven EQL-G3-associated genes, and three

**Table 2**
Summary of the G3 (VP7) lineages described in this study[a].

| G3 Lineage | Source of Lineage Designation | Bootstrap Support | Intra-Lineage Nucleotide Homology | Inter-Lineage Nucleotide Homology |
|---|---|---|---|---|
| Lineage I | Martínes-Laso et al., 2009; Stupka et al., 2009 | 99% | 89.9–99.8% | 78.8–89.5% |
| Lineage II | Martínes-Laso et al., 2009; Stupka et al., 2009[b] | 99% | 90.7–99.2% | 80.1–89.0% |
| Lineage III | Martínes-Laso et al., 2009; Stupka et al., 2009 | 100% | 96.0–98.3% | 78.9–89.2% |
| Lineage IV | Martínes-Laso et al., 2009; Stupka et al., 2009 | 100% | 94.9–96.0% | 78.8–89.1% |
| Lineage V | Chakraborty et al., 2016[c] | 100% | 93.6–99.8% | 80.1–89.5% |
| Lineage VI | Collins et al., 2008[d] | 100% | 92.5–100.0% | 80.3–89.2% |
| Lineage VII | This Study | 100% | 92.1–99.2% | 79.5–89.0% |
| Lineage VIII | This Study | 100% | 91.4–100.0% | 80.6–88.4% |
| Lineage IX | This Study | 99% | 90.4–100.0% | 80.7–88.7% |

[a] Genotype-specific, multi-parameter metrics were determined and applied to delineate these G3 lineages. The shared nucleotide identities were based on distance matrices prepared using the p-distance algorithm in MEGA6, and phylograms incorporated bootstrap testing using 1000 replicates to estimate branch support.
[b] This lineage was initially identified by referencing the included sources, however, was subsequently revised to satisfy the multi-parameter metrics applied to revise and identify the G3 lineages reported in this study.
[c] Revised from lineage I (Chakraborty et al., 2016) to lineage V in this study.
[d] Revised from lineages G3A and G3B (Collins et al., 2008) to lineage VI in this study.

genogroup-2 genes that exhibited the greatest genetic similarity with locally circulating G2P[4] strains (Figs. 2, 3B, 4A, 5A–5D, S1A–S1K); therefore, this strain was likely derived from reassortment(s) of an EQL-G3P[8] and G2P[4] strains in local circulation. Our results for mixed infection strain DOM-3705 (G1G3P[6]P[8]) did not allow for identification of the parental strains; however, WGA for DOM-3705-A and DOM-3705-B suggest that DOM-3705 resulted from co-infection involving a Wa-like G1-P[8]-I1-R1-C1-M1-A1-N1-T1-E1-H1 strain and an EQL-G3P[6] strain (G3-P[6]-I2-R2-C2-M2-A2-N2-T2-E2-H2) in local circulation. If so, the EQL-G3P[6] may have been derived from reassortment of an EQL-G3P[8] and a typical G3P[6] strain, known to exist in local circulation. However, additional RVA surveillance among human populations in the DOM is required to further elucidate the origins of novel EQL-G3P[8] strains derived from local reassortment events.

Genetic analyses involving a dynamic subset of G3 (VP7) sequences deposited into GenBank thus far, including those from the DOM described here, led to the new delineation of G3 lineages I–IX (Figs. 3A and S1A and Table 2). The interior partitioning observed within G3 lineage IX (Figs. 3A and S1A) is attributed to the lesser sequence similarity shared between the EQL-G3 strains and ancestral equine strain Erv105 (90.4–91.1% [96.9–97.9%]). Novel G3 lineage VII was comprised animal strains, including bovine-, equine-, and bat-strains (Figs. 3A and S1A and Table 1). Lineage II was revised from previous descriptions (Martinez-Laso et al., 2009; Stupka et al., 2009), such that strains RVA/Simian-tc/USA/RRV/1975/G3P[3] and RVA/Dog-tc/ITA/RV52-96/1996/G3P[3] remained within the newly delineated lineage II, while strain RVA/Human-wt/THA/CMH222/2001/G3P[3], previously classified within lineage II, exhibited greater genetic similarity with a cluster of strains described here as novel lineage VIII (Figs. 3A and S1A). Lineage I as described previously (Chakraborty et al., 2016) was re-designated here as lineage V to preserve the integrity of earlier, more universally accepted lineage I descriptions (Figs. 3A and S1A) (Martinez-Laso et al., 2009; Stupka et al., 2009), and previously described equine lineages G3A and G3B (Collins et al., 2008) were combined and re-designated here as lineage VI (Figs. 3A and S1A). Lineages I, III, and IV remained as described previously (Figs. 3A and S1A) (Martinez-Laso et al., 2009; Stupka et al., 2009). The G3 lineage delineations described here provide valuable data to better understand the contemporary diversity among RVAs resulting from the accumulation of point mutations and genetic reassortment events.

Our results indicated minimal differences (< 3.0% aa divergence) in the encoded proteins across all 11 gene segments among the EQL-G3 study strains and when compared against the larger set of reported EQL-G3 strains (Fig. 6 and Tables 1–2, S2). Analyses comparing the aa sequence differences observed among each EQL-G3 study strain and the other previously reported EQL-G3 strains included in phylogenetic analyses indicated ≤3 amino acid differences across the VP7 antigenic regions (Fig. 6 and Table S2). Therefore, the EQL-G3P[8] study strains did exhibit surface exposed aa sequence differences within the VP7 antigenic regions; however, only minimal differences were observed most which involved conservative or moderate aa substitutions (Fig. 6). Nevertheless, we recommend in-depth future study investigating the functional changes that exist among these emergent atypical G3 strains, specifically potential vaccine escape mutations.

Atypical double and triple IGR EQL-G3 strains were identified in children residing in the DOM, varying from 5 months of age through 5 years of age. These strains were first collected from 1-year-olds on November 11th, 2014 and April 14th, 2015 at the Santiago and Santo Domingo sites, respectively. During the 2015 season, EQL-G3 genotypes were identified in ten specimens accounting for 38% of the RVA strains collected that season (Fig. 1A–B). EQL-G3 strains also predominated the 2016 season and increased in prevalence, identified in thirteen specimens accounting for 62% of the RVA infections collected that season (Fig. 1A–B). Although this study only includes surveillance data across two RVA seasons, our results indicate short-term endemic circulation of EGL-G3 strains in the DOM. Additional RVA surveillance in the DOM is recommended to further monitor the prevalence of these endemic IGR strains.

Previous studies investigating the emergence of EQL-G3 strains have all included G3 sequences that shared the greatest nt identity (outside of themselves) with equine-strain Erv105. Naturally, most of these studies have indicated the EQL-G3 strains were of equine origin. Interestingly, strain Erv105 is the only RVA strain, equine or otherwise, with complete coding sequence deposited into the GenBank database exhibiting > 90% shared nt identity with any of the EQL-G3 strains reported thus far. Furthermore, for strain Erv105 the VP7 sequence was the only sequence deposited into GenBank, which was generated as part of published study that was subsequently retracted (https://www.ncbi.nlm.nih.gov/pmc/articles/PMC1932979/); although the retraction notice made no statement suggesting submission of erroneous VP7 sequence for strain Erv105. Lastly, according to sequences deposited into the GenBank database thus far, the highest shared nt identity between strain Erv105 and any other equine strain is 87%. These results may indicate that strain Erv105 is less likely of equine origin but rather was derived from some alternative mechanism(s) of origin (e.g. a human RVA G3 strain that infected a member of the equine family). Therefore, we suggest continued RVA surveillance of human and equine populations to help to elucidate the definitive origin of these emergent, human reassortant RVAs possessing a novel G3 genotype.

Since 2013, the rapid emergence and spread of EQL-G3 strains has been anecdotally attributed to Rotarix-induced selective pressure. Interestingly, a recent study including analysis of two decades of Australian surveillance data found that G1P[8] strains dominated the

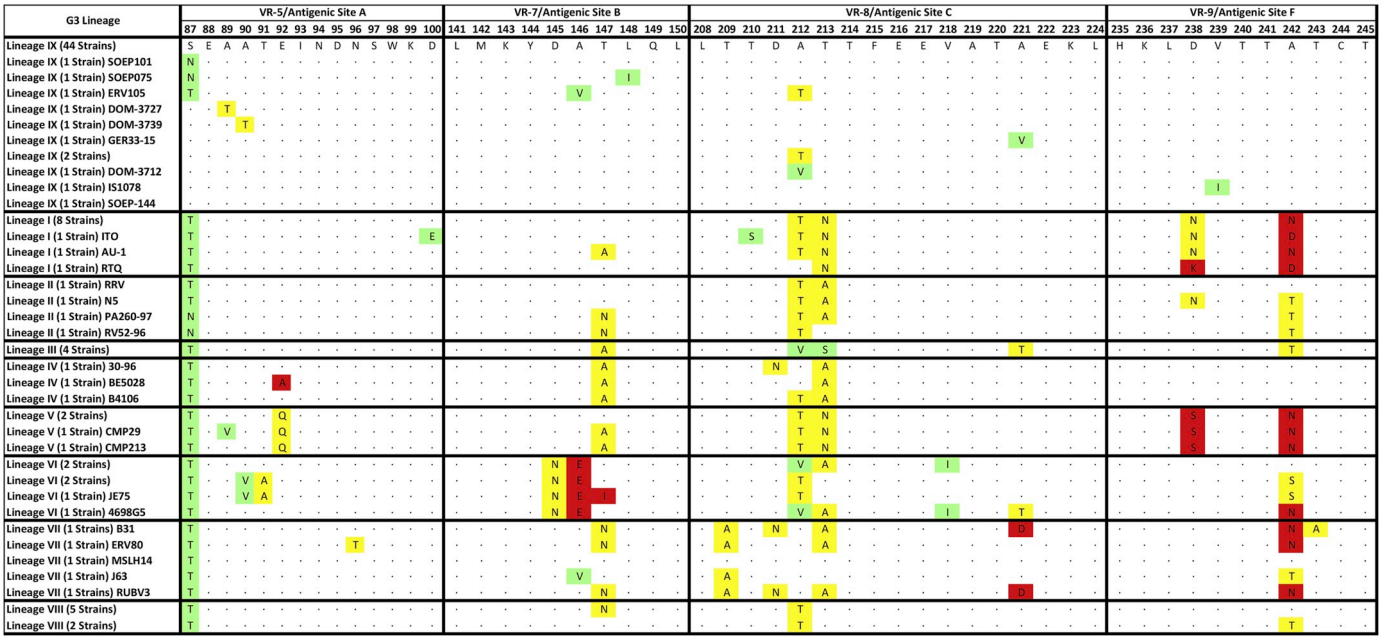


**Fig. 6.** A summary of the amino acid sequences across the VP7 antigenic regions A, B, C, and F for all G3 RVA strains included in phylogenetic analyses; including those exhibiting conservative- (green), moderate- (yellow), and radical- (red) aa substitutions.

pre-vaccine era (1995–2006), while following vaccine introduction (2007–2015) genotype distribution varied based on localized vaccine use, with G12P[8] strains dominant in areas using RotaTeq, and EQL-G3P[8] and G2P[4] strains dominant in areas using Rotarix (Roczo-Farkas et al., 2018). Roczo-Farkas et al., suggested that both RVA vaccines exerted different immunological pressures that influenced the diversity of RVA strains circulating in Australia (Roczo-Farkas et al., 2018). Rotarix was introduced into the DOM's NIP in 2012 and our results confirm the emergence of EQL-G3P[8] strains no later than November 2014. The DOM was one of the first countries to approve licensure for use of Rotarix in 2004 (Dennehy, 2008), therefore the DOM could prove an ideal candidate to investigate post-Rotarix-licensure strain ecology. Although RVA surveillance of specimens collected post-Rotarix introduction from the DOM prior to 2014 could benefit studies investigating vaccine-induced selective pressure, such specimens may not be available. In addition, if EQL-G3P[8] strains were indeed introduced into the DOM through virus dispersal from another country, such as Thailand, access to older specimens from the DOM may not indicate the emergence of EQL-G3P[8] strains prior to those identified here. Our results are consistent with the hypothesis that existence of EQL-G3 strains in the DOM may be attributed to vaccine-induced immunological pressures that influence the diversity of RVAs in contemporary circulation (Roczo-Farkas et al., 2018) but the possibility that these atypical DS-1-like strains simply may have a general fitness advantage that has allowed for their increased prevalence cannot be ruled out. Further studies are needed to help to elucidate the mechanism(s) responsible for the increased prevalence of these atypical DS-1-like strains among populations using Rotarix.

This study confirmed the emergence and spread of dynamic and diverse RVA strains to the DOM. Whole-gene analysis of RVAs identified from the DOM exhibit the invaluable benefits of multi-year global RVA surveillance studies. Our results allow for a better understanding of the ubiquitous nature and diversity of RVAs, facilitate accurate interpretations to determine the origin and evolutionary patterns of a given RVA strain, and confirm the need for studies investigating the role of vaccine-induced pressure on the contemporary RVAs in circulation. The IGR events confirmed here, along with others occurring globally, may facilitate the emergence of RVA mixed genotype constellations from both human and animal viruses that could have implications for current RVA vaccination strategies.

## Declarations of interest

None.

## Disclaimer

The conclusions, findings, and opinions expressed by authors contributing to this research article do not necessarily reflect the official position of the Centers for Disease Control and Prevention, or the authors' affiliated institutions. Use of trade names is for identification only and does not imply endorsement by any of the groups named above.

## Funding source declaration

This work was funded by the Centers for Disease Control and Prevention and the World Health Organization.

## Conflicts of interest

The authors have no professional or financial conflicts of interest related to this study and its publication.

## Acknowledgments

We wish to thank Leanne Ward, Rashi Gautam, and the Rotavirus Surveillance and Molecular Epidemiology Team at the Centers for Disease Control and Prevention for their review of this manuscript and helpful comments; and the staff of the Pan American Health Organization (PAHO), the Dr. Robert Reid Cabral Children's Hospital, and the Dr. Arturo Grullón University Regional Children's Hospital, Dominican Republic for invaluable assistance.

## Appendix A. Supplementary data

Supplementary data to this article can be found online at https://doi.org/10.1016/j.virol.2019.06.007.

## References


Altschul, S.F., Gish, W., Miller, W., Myers, E.W., Lipman, D.J., 1990. Basic local alignment search tool. J. Mol. Biol. 215 (3), 403–410. https://doi.org/10.1016/s0022-2836(05)80360-2.

Arana, A., Montes, M., Jere, K.C., Alkorta, M., Iturriza-Gomara, M., Cilla, G., 2016. Emergence and spread of G3P[8] rotaviruses possessing an equine-like VP7 and a DS-1-like genetic backbone in the Basque Country (North of Spain), 2015. Infect. Genet. Evol. 44, 137–144. https://doi.org/10.1016/j.meegid.2016.06.048.

Araujo, I.T., Assis, R.M., Fialho, A.M., Mascarenhas, J.D., Heinemann, M.B., Leite, J.P., 2007. Brazilian P[8],G1, P[8],G5, P[8],G9, and P[4],G2 rotavirus strains: nucleotide sequence and phylogenetic analysis. J. Med. Virol. 79 (7), 995–1001. https://doi.org/10.1002/jmv.20918.

Bourdett-Stanziola, L., Jimenez, C., Ortega-Barria, E., 2008. Diversity of human rotavirus G and P genotypes in Panama, Costa Rica, and the Dominican Republic. Am. J. Trop. Med. Hyg. 79 (6), 921–924. http://www.ncbi.nlm.nih.gov/pubmed/19052306.

Bourdett-Stanziola, L., Ortega-Barria, E., Espinoza, F., Bucardo, F., Jimenez, C., Ferrera, A., 2011. Rotavirus genotypes in Costa Rica, Nicaragua, Honduras and the Dominican republic. Intervirology 54 (1), 49–52. https://doi.org/10.1159/000318863.

Chakraborty, P., Bhattacharjee, M.J., Sharma, I., Pandey, P., Barman, N.N., 2016. Unusual rotavirus genotypes in humans and animals with acute diarrhoea in Northeast India. Epidemiol. Infect. 144 (13), 2780–2789. https://doi.org/10.1017/s0950268816000807.

Chavers, T.P., de Oliveira, L.H., Parashar, U.D., Tate, J.E., 2018. Post-Licensure experience with rotavirus vaccination in Latin America and the Caribbean: a systematic review and meta-analysis. Expert Rev. Vaccines. https://doi.org/10.1080/14760584.2018.1541409.

Ciarlet, M., Hoshino, Y., Liprandi, F., 1997. Single point mutations may affect the serotype reactivity of serotype G11 porcine rotavirus strains: a widening spectrum? J. Virol. 71 (11), 8213–8220. http://www.ncbi.nlm.nih.gov/pubmed/9343172.

Collins, P.J., Cullinane, A., Martella, V., O'Shea, H., 2008. Molecular characterization of equine rotavirus in Ireland. J. Clin. Microbiol. 46 (10), 3346–3354. https://doi.org/10.1128/JCM.00995-08.

Cowley, D., Donato, C.M., Roczo-Farkas, S., Kirkwood, C.D., 2016. Emergence of a novel equine-like G3P[8] inter-genogroup reassortant rotavirus strain associated with gastroenteritis in Australian children. J. Gen. Virol. 97 (2), 403–410. https://doi.org/10.1099/jgv.0.000352.

de Oliveira, L.H., Danovaro-Holliday, M.C., Andrus, J.K., de Fillipis, A.M., Gentsch, J., Matus, C.R., ... Rotavirus Surveillance, N., 2009. Sentinel hospital surveillance for rotavirus in Latin american and Caribbean countries. J. Infect. Dis. 200 (Suppl. 1), S131–S139. https://doi.org/10.1086/605060.

Dennehy, P.H., 2008. Rotavirus vaccines: an overview. Clin. Microbiol. Rev. 21 (1), 198–208. https://doi.org/10.1128/CMR.00029-07.

Diaz-Ruiz, J.R., Kaper, J.M., 1978. Isolation of viral double-stranded RNAs using a LiCl fractionation procedure. Prep. Biochem. 8 (1), 1–17. https://doi.org/10.1080/00327487808068215.

Dóró, R., Marton, S., Bartókné, A.H., Lengyel, G., Agócs, Z., Jakab, F., Bányai, K., 2016. Equine-like G3 rotavirus in Hungary, 2015–Is it a novel intergenogroup reassortant pandemic strain? Acta Microbiol. Immunol. Hung. 63 (2), 243–255.

Dyall-Smith, M.L., Lazdins, I., Tregear, G.W., Holmes, I.H., 1986. Location of the major antigenic sites involved in rotavirus serotype-specific neutralization. Proc. Natl. Acad. Sci. U. S. A. 83 (10), 3465–3468. http://www.ncbi.nlm.nih.gov/pubmed/2422651.

Edgar, R.C., 2004. MUSCLE: a multiple sequence alignment method with reduced time and space complexity. BMC Bioinf. 5, 113. https://doi.org/10.1186/1471-2105-5-113.

Esona, M.D., McDonald, S., Kamili, S., Kerin, T., Gautam, R., Bowen, M.D., 2013. Comparative evaluation of commercially available manual and automated nucleic acid extraction methods for rotavirus RNA detection in stools. J. Virol Methods 194 (1–2), 242–249. https://doi.org/10.1016/j.jviromet.2013.08.023.

Esona, M.D., Buteau, J., Lucien, M.A., Joseph, G.A., Leshem, E., Boncy, J., ... Balajee, S.A., 2015a. Rotavirus group A genotypes detected through diarrheal disease surveillance in Haiti, 2012. Am. J. Trop. Med. Hyg. 93 (1), 54–56. https://doi.org/10.4269/ajtmh.14-0403.

Esona, M.D., Gautam, R., Tam, K.I., Williams, A., Mijatovic-Rustempasic, S., Bowen, M.D., 2015b. Multiplexed one-step RT-PCR VP7 and VP4 genotyping assays for rotaviruses using updated primers. J. Virol Methods 223, 96–104. https://doi.org/10.1016/j.jviromet.2015.07.012.

Esona, M.D., Roy, S., Rungsrisuriyachai, K., Sanchez, J., Vasquez, L., Gomez, V., ... Vazquez, M., 2017. Characterization of a triple-recombinant, reassortant rotavirus strain from the Dominican Republic. J. Gen. Virol. 98 (2), 134–142. https://doi.org/10.1099/jgv.0.000688.

Esona, M.D., Roy, S., Rungsrisuriyachai, K., Gautam, R., Hermelijn, S., Rey-Benito, G., Bowen, M.D., 2018. Molecular characterization of a human G20P[28] rotavirus a strain with multiple genes related to bat rotaviruses. Infect. Genet. Evol. 57, 166–170. https://doi.org/10.1016/j.meegid.2017.11.025.

Esteban, L.E., Rota, R.P., Gentsch, J.R., Jiang, B., Esona, M., Glass, R.I., ... Castello, A.A., 2010. Molecular epidemiology of group A rotavirus in Buenos Aires, Argentina 2004-2007: reemergence of G2P[4] and emergence of G9P[8] strains. J. Med. Virol. 82 (6), 1083–1093. https://doi.org/10.1002/jmv.21745.

Estes, M., Greenberg, H., 2013. Rotaviruses. In: sixth ed. In: Fields, B.N., Knipe, D.M., Howley, P.M. (Eds.), Fields Virology, vol. 2. Wolters Kluwer Health/Lippincott Williams & Wilkins, Philadelphia, pp. 1347–1401.

Freeman, M.M., Kerin, T., Hull, J., McCaustland, K., Gentsch, J., 2008. Enhancement of detection and quantification of rotavirus in stool using a modified real-time RT-PCR assay. J. Med. Virol. 80 (8), 1489–1496. https://doi.org/10.1002/jmv.21228.

Fujii, Y., Nakagomi, T., Nishimura, A., Noguchi, A., Miura, S., Ito, H., ... Nakagomi, O., 2014. Spread and predominance in Japan of novel G1P [8] double-reassortant rotavirus strains possessing a DS-1-like genotype constellation typical of G2P [4] strains. Infect. Genet. Evol. 28, 426–433. https://doi.org/10.1016/j.meegid.2014.08.001.

Gautam, R., Mijatovic-Rustempasic, S., Esona, M.D., Tam, K.I., Quaye, O., Bowen, M.D., 2016. One-step multiplex real-time RT-PCR assay for detecting and genotyping wild-type group A rotavirus strains and vaccine strains (Rotarix(R) and RotaTeq(R)) in stool samples. PeerJ 4https://doi.org/10.7717/peerj.1560. e1560.

GBD 2016 Diarrhoeal Disease Collaborators, 2018. Estimates of the global, regional, and national morbidity, mortality, and aetiologies of diarrhoea in 195 countries: a systematic analysis for the Global Burden of Disease Study 2016. Lancet Infect. Dis. https://doi.org/10.1016/s1473-3099(18)30362-1.

Gentsch, J.R., Glass, R.I., Woods, P., Gouvea, V., Gorziglia, M., Flores, J., ... Bhan, M.K., 1992. Identification of group A rotavirus gene 4 types by polymerase chain reaction. J. Clin. Microbiol. 30 (6), 1365–1373. http://www.ncbi.nlm.nih.gov/pubmed/1320625.

Ghosh, S., Kobayashi, N., 2011. Whole-genomic analysis of rotavirus strains: current status and future prospects. Future Microbiol. 6 (9), 1049–1065. https://doi.org/10.2217/fmb.11.90.

Ghosh, S., Adachi, N., Gatheru, Z., Nyangao, J., Yamamoto, D., Ishino, M., ... Kobayashi, N., 2011. Whole-genome analysis reveals the complex evolutionary dynamics of Kenyan G2P[4] human rotavirus strains. J. Gen. Virol. 92 (Pt 9), 2201–2208. https://doi.org/10.1099/vir.0.033001-0.

Guerra, S.F., Soares, L.S., Lobo, P.S., Penha Junior, E.T., Sousa Junior, E.C., Bezerra, D.A., ... Mascarenhas, J.D., 2016. Detection of a novel equine-like G3 rotavirus associated with acute gastroenteritis in Brazil. J. Gen. Virol. 97 (12), 3131–3138. https://doi.org/10.1099/jgv.0.000626.

Henikoff, S., Henikoff, J.G., 1992. Amino acid substitution matrices from protein blocks. Proc. Natl. Acad. Sci. U. S. A. 89 (22), 10915–10919. https://doi.org/10.1073/pnas.89.22.10915.

Hoa-Tran, T.N., Nakagomi, T., Vu, H.M., Do, L.P., Gauchan, P., Agbemabiese, C.A., ... Thanh, N.T., 2016. Abrupt emergence and predominance in Vietnam of rotavirus A strains possessing a bovine-like G8 on a DS-1-like background. Arch. Virol. 161 (2), 479–482. https://doi.org/10.1007/s00705-015-2682-x.

Hurvich, C.M., Tsai, C.-L., 1989. Regression and time series model selection in small samples. Biometrika 76 (2), 297–307. https://doi.org/10.1093/biomet/76.2.297.

Jere, K.C., Chaguza, C., Bar-Zeev, N., Lowe, J., Peno, C., Kumwenda, B., ... Iturriza-Gomara, M., 2018. Emergence of double- and triple-gene reassortant G1P[8] rotaviruses possessing a DS-1-like backbone after rotavirus vaccine introduction in Malawi. J. Virol. 92 (3). https://doi.org/10.1128/jvi.01246-17.

Katz, E.M., Gautam, R., Bowen, M.D., 2017. Evaluation of an alternative recombinant thermostable thermus thermophilus (rTth)-Based real-time reverse transcription-PCR kit for detection of rotavirus A. J. Clin. Microbiol. 55 (5), 1585–1587. https://doi.org/10.1128/jcm.00126-17.

Khamrin, P., Peerakome, S., Tonusin, S., Malasao, R., Okitsu, S., Mizuguchi, M., ... Maneekarn, N., 2007. Changing pattern of rotavirus G genotype distribution in Chiang Mai, Thailand from 2002 to 2004: decline of G9 and reemergence of G1 and G2. J. Med. Virol. 79 (11), 1775–1782. https://doi.org/10.1002/jmv.20960.

Kirkwood, C.D., Roczo-Farkas, S., 2014. Australian rotavirus surveillance program annual report, 2013. Comm. Dis. Intell. 38 (4), E334–E342.

Kirkwood, C.D., Boniface, K., Barnes, G.L., Bishop, R.F., 2011. Distribution of rotavirus genotypes after introduction of rotavirus vaccines, Rotarix(R) and RotaTeq(R), into the national immunization program of Australia. Pediatr. Infect. Dis. J. 30 (1 Suppl. l), S48–S53. https://doi.org/10.1097/INF.0b013e3181fefd90.

Komoto, S., Tacharoenmuang, R., Guntapong, R., Ide, T., Haga, K., Katayama, K., ... Taniguchi, K., 2015. Emergence and characterization of unusual DS-1-like G1P[8] rotavirus strains in children with diarrhea in Thailand. PLoS One 10 (11). https://doi.org/10.1371/journal.pone.0141739. e0141739.

Komoto, S., Tacharoenmuang, R., Guntapong, R., Ide, T., Tsuji, T., Yoshikawa, T., ... Taniguchi, K., 2016. Reassortment of human and animal rotavirus gene segments in emerging DS-1-like G1P[8] rotavirus strains. PLoS One 11 (2). https://doi.org/10.1371/journal.pone.0148416. e0148416.

Komoto, S., Ide, T., Negoro, M., Tanaka, T., Asada, K., Umemoto, M., ... Taniguchi, K., 2018. Characterization of unusual DS-1-like G3P[8] rotavirus strains in children with diarrhea in Japan. J. Med. Virol. 90 (5), 890–898. https://doi.org/10.1002/jmv.25016.

Le, V.P., Chung, Y.C., Kim, K., Chung, S.I., Lim, I., Kim, W., 2010. Genetic variation of prevalent G1P[8] human rotaviruses in South Korea. J. Med. Virol. 82 (5), 886–896. https://doi.org/10.1002/jmv.21653.

Luchs, A., Cilli, A., Morillo, S., Boen, L., Carmona, R.D.C., Timenetsky, M.D.C.S.T., 2018. Spread of the emerging equine-like G3P[8] DS-1-like genetic backbone rotavirus strain in Brazil. Int. J. Infect. Dis. 73, 190. https://doi.org/10.1016/j.ijid.2018.04.3845.

Maes, P., Matthijnssens, J., Rahman, M., Van Ranst, M., 2009. RotaC: a web-based tool for the complete genome classification of group A rotaviruses. BMC Microbiol. 9, 238. https://doi.org/10.1186/1471-2180-9-238.

Malasao, R., Saito, M., Suzuki, A., Imagawa, T., Nukiwa-Soma, N., Tohma, K., ... Oshitani, H., 2015. Human G3P[4] rotavirus obtained in Japan, 2013, possibly emerged through a human-equine rotavirus reassortment event. Virus Gene. 50 (1), 129–133. https://doi.org/10.1007/s11262-014-1135-z.

Martinez-Laso, J., Roman, A., Rodriguez, M., Cervera, I., Head, J., Rodriguez-Avial, I., Picazo, J.J., 2009. Diversity of the G3 genes of human rotaviruses in isolates from Spain from 2004 to 2006: cross-species transmission and inter-genotype recombination generates alleles. J. Gen. Virol. 90 (Pt 4), 935–943. https://doi.org/10.

1099/vir.0.007807-0.
Mascarenhas, J.D., Lima, C.S., de Oliveira, D.S., Guerra Sde, F., Maestri, R.P., Gabbay, Y.B., ... Bensabath, G., 2010. Identification of two sublineages of genotype G2 rotavirus among diarrheic children in Parauapebas, Southern Para State, Brazil. J. Med. Virol. 82 (4), 712–719. https://doi.org/10.1002/jmv.21735.
Matthijnssens, J., Ciarlet, M., Rahman, M., Attoui, H., Bányai, K., Estes, M.K., ... Van Ranst, M., 2008a. Recommendations for the classification of group A rotaviruses using all 11 genomic RNA segments. Arch. Virol. 153 (8), 1621–1629. https://doi.org/10.1007/s00705-008-0155-1.
Matthijnssens, J., Ciarlet, M., Heiman, E., Arijs, I., Delbeke, T., McDonald, S.M., ... Van Ranst, M., 2008b. Full genome-based classification of rotaviruses reveals a common origin between human Wa-Like and porcine rotavirus strains and human DS-1-like and bovine rotavirus strains. J. Virol. 82 (7), 3204–3219. https://doi.org/10.1128/JVI.02257-07.
McDonald, S.M., Matthijnssens, J., McAllen, J.K., Hine, E., Overton, L., Wang, S., ... Patton, J.T., 2009. Evolutionary dynamics of human rotaviruses: balancing reassortment with preferred genome constellations. PLoS Pathog. 5 (10), e1000634. https://doi.org/10.1371/journal.ppat.1000634.
Mijatovic-Rustempasic, S., Frace, M.A., Bowen, M.D., 2012. Effective paramagnetic bead technique for purification of cycle sequencing products. Sequencing, 2012. https://doi.org/10.1155/2012/767959.
Mijatovic-Rustempasic, S., Roy, S., Teel, E.N., Weinberg, G.A., Payne, D.C., Parashar, U.D., Bowen, M.D., 2016. Full genome characterization of the first G3P[24] rotavirus strain detected in humans provides evidence of interspecies reassortment and mutational saturation in the VP7 gene. J. Gen. Virol. 97 (2), 389–402. https://doi.org/10.1099/jgv.0.000349.
Nakagomi, T., Nguyen, M.Q., Gauchan, P., Agbemabiese, C.A., Kaneko, M., Do, L.P., ... Nakagomi, O., 2017. Evolution of DS-1-like G1P[8] double-gene reassortant rotavirus A strains causing gastroenteritis in children in Vietnam in 2012/2013. Arch. Virol. 162 (3), 739–748. https://doi.org/10.1007/s00705-016-3155-6.
Nishikawa, K., Hoshino, Y., Taniguchi, K., Green, K.Y., Greenberg, H.B., Kapikian, A.Z., ... Gorziglia, M., 1989. Rotavirus VP7 neutralization epitopes of serotype 3 strains. Virology 171 (2), 503–515. http://www.ncbi.nlm.nih.gov/pubmed/2474892.
O'Ryan, M., 2007. Rotarix (RIX4414): an oral human rotavirus vaccine. Expert Rev. Vaccines 6 (1), 11–19. https://doi.org/10.1586/14760584.6.1.110.
Pan American Health Organization, 2012. Immunization Newsletter, vol. 34 4. https://www.paho.org/hq/index.php?option=com_content&view=article&id=6187&Itemid=40470&lang=en.
Parra, G.I., Bok, K., Martinez, V., Russomando, G., Gomez, J., 2005. Molecular characterization and genetic variation of the VP7 gene of human rotaviruses isolated in Paraguay. J. Med. Virol. 77 (4), 579–586. https://doi.org/10.1002/jmv.20495.
PATH, 2016. Country national immunization program (NIP) introductions of rotavirus vaccine. http://www.vaccineresources.org/files/PATH-Country-Introduction-Table-EN-2016.05.01.pdf.
Perkins, C., Mijatovic-Rustempasic, S., Ward, M.L., Cortese, M.M., Bowen, M.D., 2017. Genomic characterization of the first equine-like G3P[8] rotavirus strain detected in the United States. Genome Announc. 5 (47). https://doi.org/10.1128/genomeA.01341-17.
Phan, T.G., Khamrin, P., Quang, T.D., Dey, S.K., Takanashi, S., Okitsu, S., ... Ushijima, H., 2007. Detection and genetic characterization of group A rotavirus strains circulating among children with acute gastroenteritis in Japan. J. Virol. 81 (9), 4645–4653. https://doi.org/10.1128/JVI.02342-06.
Pietsch, C., Liebert, U.G., 2018. Molecular characterization of different equine-like G3 rotavirus strains from Germany. Infect. Genet. Evol. 57, 46–50. https://doi.org/10.1016/j.meegid.2017.11.007.
Ramig, R.F., 1997. Genetics of the rotaviruses. Annu. Rev. Microbiol. 51, 225–255. https://doi.org/10.1146/annurev.micro.51.1.225.
Roczo-Farkas, S., Kirkwood, C.D., Cowley, D., Barnes, G.L., Bishop, R.F., Bogdanovic-Sakran, N., ... Bines, J.E., 2018. The impact of rotavirus vaccines on genotype diversity: a comprehensive analysis of 2 decades of Australian surveillance data. J. Infect. Dis. 218 (4), 546–554. https://doi.org/10.1093/infdis/jiy197.
Santos, V.S., Marques, D.P., Martins-Filho, P.R., Cuevas, L.E., Gurgel, R.Q., 2016. Effectiveness of rotavirus vaccines against rotavirus infection and hospitalization in Latin America: systematic review and meta-analysis. Infect. Dis. Poverty 5 (1), 83. https://doi.org/10.1186/s40249-016-0173-2.
Stupka, J.A., Carvalho, P., Amarilla, A.A., Massana, M., Parra, G.I., Argentinean National Surveillance Network for, D, 2009. National Rotavirus Surveillance in Argentina: high incidence of G9P[8] strains and detection of G4P[6] strains with porcine characteristics. Infect. Genet. Evol. 9 (6), 1225–1231. https://doi.org/10.1016/j.meegid.2009.07.002.
Tacharoenmuang, R., Komoto, S., Guntapong, R., Ide, T., Sinchai, P., Upachai, S., ... Taniguchi, K., 2016. Full genome characterization of novel DS-1-like G8P[8] rotavirus strains that have emerged in Thailand: reassortment of bovine and human rotavirus gene segments in emerging DS-1-like intergenogroup reassortant strains. PLoS One 11 (11). https://doi.org/10.1371/journal.pone.0165826. e0165826.
Tamura, K., Stecher, G., Peterson, D., Filipski, A., Kumar, S., 2013. MEGA6: molecular evolutionary genetics analysis version 6.0. Mol. Biol. Evol. 30 (12), 2725–2729. https://doi.org/10.1093/molbev/mst197.
Trinh, Q.D., Pham, N.T., Nguyen, T.A., Phan, T.G., Yan, H., Hoang le, P., ... Ushijima, H., 2010. Sequence analysis of the VP7 gene of human rotaviruses G2 and G4 isolated in Japan, China, Thailand, and Vietnam during 2001-2003. J. Med. Virol. 82 (5), 878–885. https://doi.org/10.1002/jmv.21630.
Troeger, C., Khalil, I.A., Rao, P.C., Cao, S., Blacker, B.F., Ahmed, T., ... Reiner Jr., R.C., 2018. Rotavirus vaccination and the global burden of rotavirus diarrhea among children younger than 5 years. JAMA Pediatr. 172 (10), 958–965. https://doi.org/10.1001/jamapediatrics.2018.1960.
Utsumi, T., Wahyuni, R.M., Doan, Y.H., Dinana, Z., Soegijanto, S., Fujii, Y., ... Shoji, I., 2018. Equine-like G3 rotavirus strains as predominant strains among children in Indonesia in 2015-2016. Infect. Genet. Evol. 61, 224–228. https://doi.org/10.1016/j.meegid.2018.03.027.
Velazquez, R.F., Linhares, A.C., Munoz, S., Seron, P., Lorca, P., DeAntonio, R., Ortega-Barria, E., 2017. Efficacy, safety and effectiveness of licensed rotavirus vaccines: a systematic review and meta-analysis for Latin America and the Caribbean. BMC Pediatr. 17 (1), 14. https://doi.org/10.1186/s12887-016-0771-y.
WHO Coordinated Rotavirus Surveillance Network, 2012. RV surveillance case definitions. http://www.who.int/immunization/monitoring_surveillance/resources/RV_Case_Defs.pdf.
World Health Organization, 2016. Child Rotavirus Deaths by Country: 2013. www.who.int/immunization/monitoring_surveillance/burden/estimates/rotavirus/en/.
Yamamoto, S.P., Kaida, A., Kubo, H., Iritani, N., 2014. Gastroenteritis outbreaks caused by a DS-1-like G1P[8] rotavirus strain, Japan, 2012-2013. Emerg. Infect. Dis. 20 (6), 1030–1033. https://doi.org/10.3201/eid2006.131326.
Yamamoto, D., Tandoc 3rd, A., Mercado, E., Quicho, F., Lupisan, S., Obata-Saito, M., ... Oshitani, H., 2017. First detection of DS-1-like G1P[8] human rotavirus strains from children with diarrhoea in the Philippines. New Microb. New Infect. 18, 54–57. https://doi.org/10.1016/j.nmni.2017.04.001.